

**Electrochemical Redox Process Analysis of Cu^{+2} and Fe^{+3} ions in Natural Waters
Using Cyclic Voltammetry Technique**

By
Iris E. Suero De Jesús

A Thesis submitted in partial fulfillment of the requirements for the degree of

MASTER IN SCIENCE
CHEMISTRY

UNIVERSITY OF PUERTO RICO
MAYAGÜEZ CAMPUS
DECEMBER 2012

Approved by:

Carmen A. Vega, Ph.D.
President, Graduate Committee

Date

Aidalu Joubert, Ph.D.
Member, Graduate Committee

Date

Juan López-Garriga, Ph.D.
Member, Graduate Committee

Date

Miriam J. Nieto, Ph.D.
Rep. Graduate School

Date

Rene S. Vieta, Ph.D.
Director of Department

Date

Summary

The concentration and distribution of trace metals in natural water is important in order to have a better understanding of their biogeochemical behavior and natural cycles. This biological behavior and natural cycles are associated with the global warming effect, which is one of the most important concerns for scientists these days. Copper (Cu) and Iron (Fe) are important trace metals in natural waters. Copper (Cu) and Iron (Fe) are found in nature in the oxidation state of Cu (II)/Cu (I) and Fe (III)/ Fe (II). Recent researches have determined that Cu can exist in the oxidation state (I), which is lethal to microorganism when the concentration exceeds the Environmental Standard Quality of 5 $\mu\text{g/L}$ (annual average). Hydrogen peroxide (H_2O_2), a strong reductant agent, formed in natural water by the interaction with the ultra-violet light react causing the reduction of Cu (II) to form Cu (I). The oxidation-reduction process of these elements has been studied using UV- Vis Spectrophotometric system, Cathodic Stripping Voltametry, Colorimetric technique and Quimioluminescence. However, Cyclic Voltammetry (CV) is a very fast, accessible and economic analytical technique that can be used for the analysis of trace metal in natural waters. The effectiveness of CV results from its capacity for rapidly observing the reduction-oxidation (redox) behavior of analytes over a wide potential range applied. Our research was focus on the development of an experimental design for the determination of these elements, Cu (II) and Fe (III), using standard addition method by Cyclic Voltammetry. Consequently, the optimization of the following instrumental parameters: Working electrode, Potential Window, Scan Rate and Sensitivity. Our results indicate that the levels of Cu (II) and Fe (III) ions concentration in the seawater of Mayaguez coast were 7.7 (± 1) μM and 1.7 (± 0.4) μM , respectively. The pH and salinity measured of the seawater of Mayaguez, P.R. were 8.07 and 26.42 mgL^{-1} , respectively.

Resumen

Es importante conocer la concentración y distribución de los metales a nivel traza en aguas naturales para poder tener mejor entendimiento de su comportamiento biogeoquímico y ciclo natural. El comportamiento biológico y los ciclos naturales están asociados al efecto de calentamiento global, el cual es uno de las preocupaciones de los científicos en estos días. Cobre (Cu) y Hierro (Fe) se encuentran en la naturales en sus estados de oxidación Cu (II)/Cu (I), y Fe (III)/Fe (II). Investigaciones recientes han determinado que Cu puede existir en su estado de oxidación (I), el cual es letal a los microorganismos cuando se excede el Estándar de Calidad Ambiental de 5 µg/L en un promedio anual. El peróxido de hidrogeno (H₂O₂) es un agente reductor fuerte que se forma en las aguas naturales por la interacción con la luz ultravioleta ocasionando la reducción de Cu (II) para formar Cu (I). Las siguientes técnicas han sido utilizadas para el análisis de metales trace en aguas naturales: Espectrofotometría, “Stripping Voltammetry”, Técnicas Colorimétricas y Quimioluminiscencia. Sin embargo, la técnica de Voltametría Cíclica (CV) es bien rápida, accesible y económica técnica analítica que puede ser utilizada para el análisis de metales traza en aguas naturales. La efectividad de CV resulta de su capacidad para observar rápidamente el comportamiento de oxidación-reducción de los analitos sobre un amplio rango de potencial aplicado. Nuestro trabajo se enfoca en la desarrollo de un modelo experimental para cuantificar los iones de Cu (II) y Fe (III) utilizando la técnica de Voltametría Cíclica con el Método de Adición de Estándar. Por consiguiente la optimización de los siguientes parámetros instrumentales: Electrodo de trabajo, Ventana de Potencial, Velocidad de barrido y Sensitividad. Nuestros resultados indican que los niveles de Cu (II) y Fe (III) en el agua de mar de la costa de Mayagüez, P.R. fue 7.7 (± 1) µM y 1.7 (± 0.4) µM, respectivamente.

The following work is dedicated to:
my mom, and to my nephews;
Gianyris, Dylan and Yadriel.

Symbols and Abbreviations

A	Ampere(s)
AE	Auxiliary electrode
Ag	Silver
AgCl	Silver chloride
BAS	Bioanalytical Systems
C_R^*	Bulk concentration of the reduced species
CTFE	CTFE - Chlorotrifluoroethylene
Cu	Cu - Copper
CV	CV - Cyclic Voltammetry
D_R	Diffusion coefficient of the reduced species
e^-	Electron
E	Potential
E^0	Standard Potential
E_{anodic}	Anodic peak potential
E_{cathodic}	Cathodic peak potential
EC	Electrochemical
ECS	ECS- Saturated Calomel electrode
E_i	Initial potential
E_{Pa}	Anodic peak potential
E_{Pc}	Cathodic peak potential
E_s	Switching potential
F	Faraday constant
Fe	Iron
Fig.	Figure
GC	Glassy Carbon
GCE	Glassy carbon electrode
GCWE	Glassy Carbon Working Electrode
i	Current

Symbols and Abbreviations

isd	Initial scan direction
i_L	Limiting current
i_{Pa}	Anodic current
i_{Pc}	Cathodic current
K	Equilibrium constant
M	Molarity
mM	Millimolar
min	Minute(S)
mL	Milliliter(s)
mV	millivolt(S)
n	Number of electrons
NaCl	Sodium chloride
O	Oxidized species
Pt	Platimun
PtE	Platinum electrode
PtWE	Platinum Working Electrode
R	Reduced species
RE	Reference Electrode
Red	Reduction
t	t – time
t_0	initial time
ν	Scan rate
vs.	versus
WE	Working electrode
μ	Micro
μA	Micro Amperes
μL	Micro liters

List of Figures

- Figure 1 EC-Epsilon potentiostat connected to a BaSi C-3 Cell Stand.
- Figure 2 BaSi C-3 Cell Stand.
- Figure 3 a) Standard BaSi working electrode, b) Silver/Silver Chloride reference electrode RE-5B (Ag/AgCl), c) Auxiliary electrode.
- Figure 4 Triangular potential waveform for one cycle in a CV experiment.
- Figure 5 a) Typical cyclic voltammogram with polarographic scale using software for BAS5-Epsilon, b) variety of cyclic voltammograms.
- Figure 6 General pathway of a general electrode reaction of oxidized (O) and reduced (R) electroactive species.
- Figure 7 A single electrode reaction.
- Figure 8 Voltammogram of 1mM Cu^{+2} at a scan rate of 500mVs^{-1} and a sensitivity of $100\mu\text{AV}^{-1}$ with Ag/AgCl as the reference electrode and polarographic scale using software for BaSi-Epsilon.
- Figure 9 Voltammogram of an irreversible process.
- Figure 10 a) Voltammogram of the oxygen reduction in a solution saturated with air vs. Saturated Calomel Electrode (ECS) as reference electrode.
- Figure 11 a) Current-potential curve for a nernstian reaction involving two soluble species with only oxidant present initially, b) $\log[(i_l - i)/i]$ vs E for a system.
- Figure 12 A standard addition plot
- Figure 13 Gravity filtration system
- Figure 14 Vernier Chloride Ion Selective electrode and a Vernier Interface Lab Quest.

List of Figures

- Figure 15 Polishing step for working electrode: a)Wet Polishing pad before adding polish powder, b) add a small amount of polish solution (Alumina) to the wet pad, c) use smooth motion and light pressure when polishing.
- Figure 16 Arrangement of three electrode system in a fitted top from a C-e Cell.
- Figure 17 Diagram of the electrical circuitry for potential (E) and current (i)
- Figure 18 Sequence of steps for the initiation of the CV program.
- Figure 19 General CV parameters box corresponding to the BASi Epsilon EC software version 2.13.77, 2009. Bioanalytical System, Inc. showing a typical set of parameters.
- Figure 20 Cyclic voltammogram using a BASi Platinum electrode in a 0.5M H₂SO₄ solution at a scan rate of 100mVs⁻¹ and sensitivity 100μAV⁻¹
- Figure 21 Cyclic Voltammogram for a smooth Pt electrode in 0.5M H₂SO₄ solution.
- Figure 22 Voltammogram of 1mM Cu⁺² in 0.1M NaCl electrolyte supporting solution with a potential window from +650mV to +0mV at a scan rate of 100mVs⁻¹ and a sensitivity of 10μAV⁻¹ with Ag/AgCl as the reference electrode and Pt as the working electrode.
- Figure 23 Voltammogram of Pt electrode in 0.5M H₂SO₄ solution. Scan rate 100mVs⁻¹ and sensitivity 100μAV⁻¹. This electrode was previously used for the analysis of Cu⁺² in 0.1M NaCl electrolyte supporting solution
- Figure 24 Voltammogram of 1mM Fe⁺³ with a potential window from +750mV to +250mV at a scan rate of 100mVs⁻¹ and a sensitivity of 10μAV⁻¹ with Ag/AgCl as the reference electrode.
- Figure 25 Voltammogram of 1mM Fe⁺³ in 0.1M NaCl electrolyte supporting solution with a potential window from +1000mV to -600mV at a scan rate of 100mVs⁻¹ and a sensitivity of 10μAV⁻¹ with Ag/AgCl as the reference electrode and GC as working electrode

List of Figures

- Figure 27 Voltammogram of 1mM Cu^{+2} with a potential window from +300mV to -100mV at 100mVs^{-1} and a sensitivity of $100\mu\text{A}$ with Ag/AgCl as the reference electrode
- Figure 28 Voltammogram of 1mM Fe^{+3} with a potential window from +700mV to +250mV at 100mV/s and a sensitivity of $10\mu\text{AV}^{-1}$ with Ag/AgCl reference electrode and using PT working electrode.
- Figure 29 Cyclic voltammograms of a) 1 mM Cu^{+2} in 0.1M NaCl electrolyte supporting solution and b) 1mM Fe^{+3} electrolyte supporting solution at different scan rate from $10\text{mV}\cdot\text{s}^{-1}$ up to $1000\text{mV}\cdot\text{s}^{-1}$ and at sensitivity of $100\mu\text{AV}^{-1}$
- Figure 30 Effect of the scan rate on the peak height of the a) Cu^{+2} stock solution and, b) Fe^{+3} stock solution.
- Figure 31 Cyclic voltammogram of a) 1mM Cu^{+2} in 0.1M NaCl electrolyte supporting solution at a sensitivity of $100\mu\text{AV}^{-1}$ and b) 1mM Fe^{+3} in 0.1M NaCl electrolyte supporting solution at a sensitivity of $10\mu\text{AV}^{-1}$, representing the area selected to determine the number of electrons transferred.
- Figure 32 a) E_{pa} vs. $\text{Log}((i_l - i) / i)$ plot for the reduction process of 1mM Cu^{+2} in 0.1M NaCl electrolyte supporting solution. The measurement were taken against Ag/AgCl reference electrode at $100\text{mV}\cdot\text{s}^{-1}$ and $100\mu\text{AV}^{-1}$ in the +300mV to -100mV potential window b) E_{pa} vs. $\text{Log}((i_l - i) / i)$ plot for the reduction process of 1mM Fe^{+3} in 0.1M NaCl electrolyte supporting solution. The measurement were taken against Ag/AgCl reference electrode at $100\text{mV}\cdot\text{s}^{-1}$ and $10\mu\text{AV}^{-1}$ in the +700mV to +300mV potential window.
- Figure 33 Voltammogram of Seawater analysis a) at a scan rate of 100mVs^{-1} and a sensitivity of $100\mu\text{AV}^{-1}$ using GC working electrode vs. Ag/AgCl reference electrode, b) at a scan rate of 100mVs^{-1} and a sensitivity of $100\mu\text{AV}^{-1}$ using Pt working electrode vs. Ag/AgCl reference electrode
- Figure 34 Voltammogram of sea water at every addition of 5uL of 1mM Cu (II) stock solution at a scan rate of 100mVs^{-1} and a sensitivity of $1\mu\text{AV}^{-1}$ vs. Ag/AgCl as reference electrode and using CG working electrode toward a more negative direction.

List of Figures

- Figure 35 Voltammogram of sea water at every addition of 5uL of 1mM Fe (III) solution at a scan rate of 100mVs^{-1} and a sensitivity of $1\mu\text{AV}^{-1}$ vs. Ag/AgCl as reference electrode and using Pt working electrode toward a more negative direction
- Figure 36 Standard Addition plot for Cu (II) ion analysis in Mayaguez coast seawater using Cyclic Voltammetry Technique.
- Figure 37 Standard Addition plot for Fe (III) ion analysis in Mayaguez coast seawater using Cyclic Voltammetry Technique.
- Figure 38 Comparison of the standard addition method plot for Cu (II) ion in the analysis of the Mayaguez coast seawater at small variation in the cathodic current at the potential of a) 75 mV, b) 85mV and, c) 90mV, respectively.
- Figure 39 Comparison of three standard addition plot for Fe (III) ion analysis in Mayaguez coast seawater selecting the current the potential at a) 469 mV, b) 479mV and c) 489mV, respectively
- Figure 40 Standard Addition Plot of seawater analysis using 1000 μL spike of 1mM Cu (II) Stock solution.
- Figure 41 The standard addition plot for Cu (II) ion analysis in Mayaguez coast seawater at 85mV using 3 spikes addition.
- Figure 42 The standard addition plot for Fe (III) ion analysis in Mayaguez coast seawater at 479mV using 3 spikes addition.
- Figure 43 The standard addition plot for 1 μM Cu (II) stock solution at 75mV using 3 spikes addition and GC working electrode.
- Figure 44 The standard addition plot for 1 μM Fe (III) stock solution at 479mV using 3 spikes addition and Pt working electrode.

List of Tables

Table 1	List of price of four analytical techniques used for trace metal analysis.
Table 2	Rate constant for Fe^{+2} and Cu^{+} oxidation with H_2O_2 and O_2 in seawater
Table 3	Major voltammetric techniques used for trace-metal analysis and their typical concentration ranges. v = Potential scan rate (mV/s); DP = Pulse amplitude; f = Frequency; t_d = Preconcentration time; i_p = Peak current; E_p = Peak potential
Table 4	Mayaguez coast seawater parameters.
Table 5	Potential and Current of the Cu^{+2} to Cu^{+1} redox process of the ten samples studied.
Table 6	Potential and Current of the Fe^{+3} to Fe^{+2} redox processes of the ten samples studied.
Table 7	Potential and current at seven different scan rate for Cu^{+2} and Fe^{+3} ions in 0.1M NaCl electrolyte supporting solution using Cyclic Voltammetry Technique
Table 8	Peak separation ΔE_p and peak current ratio 1mM Cu^{+2} and 1mM Fe (III) in 0.1M NaCl supporting electrolyte solution.
Table 9	Potential (E_{pc}), limiting current (i_l), current (i) and required calculations to obtain $\log(\text{abs}(i_l - i)/i)$ for the reduction process of 1mM Cu^{+2} in 0.1M NaCl electrolyte supporting solution using +300mV to -100mV, Ag/AgCl reference electrode a $100\text{mV}\cdot\text{s}^{-1}$ and $100\mu\text{AV}^{-1}$.
Table 10	Potential (E_{pc}), limiting current (i_l), current (i) and required calculations to obtain $\log(\text{abs}(i_l - i)/i)$ for the reduction process of 1mM Fe^{+3} in 0.1M NaCl electrolyte supporting solution using +700mV to +300mV, Ag/AgCl reference electrode a $100\text{mV}\cdot\text{s}^{-1}$ and $100\mu\text{AV}^{-1}$.
Table 11	Summarize of the Cu (II) ion analysis using Standard Addition Method.

List of Tables

Table 12	Summarize of the Fe (III) ion analysis using Standard Addition Method.
Table 13	Average of the cathodic current for Cu (II) and Fe (III) ion analysis using standard addition method with Cyclic Voltammetry technique
Table 14	Determination of Cu (II) and Fe (III) content in three seawater sample using standard addition method with Cyclic Voltammetry technique.
Table 15	Cathodic current varying the cathodic peak location at three different potential
Table 16	Linear regression data for Cu (II) and Fe (III) ion analysis at the selected potentials.
Table 17	Summarize of the Cu (II) ion analysis using Standard Addition Method with addition of 1000 μ L of spike.
Table 18	Average results for 1 μ M Cu (II) and Fe (III) stock solution analysis.

Content

Chapter I: Overview	1
1.1 Introduction.....	1
1.2 Importance of trace metal analysis	2
1.3 Advantage of using Cyclic Voltammetry Technique for trace metal analysis	4
 Chapter II: Literature Review	 7
 Chapter III: Instrumentation	 16
3.1 Cyclic Voltammetry Instrumentation.....	16
3.1.1 Electrochemical workstation	16
3.2 Basic Principles of Cyclic Voltammetry	19
3.2.1 Factors affecting the electrode reaction rate and current	21
3.2.2 Reversible electrochemical reaction	24
3.2.3 Nernst equation	25
3.2.4 Oxygen reduction interference	26
3.2.5 Calculating the number of electrons transferred in the bulk redox reaction in the electrochemical experiments.	27
3.3 Standard addition method in the electrochemical experiments	29
 Chapter IV: Experimental Procedures	 32
4.1 Preparation of solutions	32
4.1.1 Preparation of electrolyte solution	32
4.1.2 Preparation of the stock solution	32
4.2 Sampling and pretreatment of natural waters	32
4.3 Measuring chloride concentration of the natural seawaters	33
4.4 pH determination.....	34
4.5 Nitrogen gas pretreatment	34
4.6 Pretreatment of the working electrode surface.....	34
4.7 Description of the experiments using Cyclic Voltammetry technique	35
4.7.1 Setting the instrumental parameters.....	35

Content

Chapter V: Results and Discussion	39
5.1 Natural waters parameters.....	39
5.2 Selecting the working electrode	40
5.2.1 Platinum Electrode (PtE).....	40
5.2.2 Glassy Carbon Electrode (GCE)	44
5.3 Selecting the working electrode for analysis of Cu^{+2} and Fe^{+3} ions.....	46
5.3.1 Copper (II) ion analysis	46
5.3.2 Iron (III) ion analysis.....	49
5.4 Selecting the sensitivity for the analysis of Cu^{+2} and Fe^{+3} ions.....	51
5.5 Effect of the scan rate on the Cu^{+2} and Fe^{+3} ion redox waves.....	51
5.6 Reversibility determination in the redox processes of Cu^{+2} and Fe^{+3} ions	54
5.7 Calculating the number of electrons transferred in the redox processes of Cu^{+2} and Fe^{+3} ions.....	56
5.8 Determination of Cu^{+2} and Fe^{+3} ions concentration in seawater using the Standard Addition Method with Cyclic Voltammetry Technique	60
5.9 Results Validation	66
Chapter VI: Conclusion and Recommendations	77
6.1 Conclusions	77
6.2 Recommendations for future works.....	78
Reference	79

Chapter I

1.1 Introduction

Our research was focus on the development of an experimental design for the determination of Cu (II) and Fe (III) in natural waters, using standard addition method by Cyclic Voltammetry (CV). Consequently, the optimization of the following instrumental parameters: Working electrode, Potential Window, Scan Rate and Sensitivity. CV is a potential-controlled reversal electroanalytical system. It is widely use for a variety of purposes, including fundamental studies of oxidation and reduction processes in various media, adsorption processes on surfaces, electron transfer and reaction mechanisms, kinetics of electron transfer processes, and transport, speciation, and thermodynamic properties of solvated species. This technique is very fast, accessible and not expensive. It allows the analysis of electroactive species, which are capable of the electron transfer process. Metals have this capacity and that is why these species are excellent to be analyzed by this method.

Previous studies had reported trace metal analysis of Cu (II) and Fe (III) ions using Anodic or Cathodic Stripping Voltammetry Technique. This technique is a very sensitive method for the analysis of trace concentrations of electroactive species in solution. Detection limits for metal ions at sub-ppb concentrations have been reported. In this technique the analyte is deposited onto the working electrode during a deposition step, and then oxidized during the stripping step. The current is measured during the stripping step. In the study "*Field Application of an Automated Voltammetric System for High-Resolution Studies of Trace Metal Distribution in Dynamic Estuarine and Coastal Waters*" an automated stripping voltammetry technique was used for continuous, near

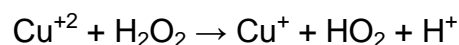
real-time monitoring of trace metals in marine systems (e.g. : [6]). Another metals such as Cu, Zn, Cd, Co, Cr and Ni had been studied in the research “Trace metal characterization in aquatic environments by Anodic Stripping Voltammetry” (e.g. : [8]). Also, the oxidation-reduction process of these elements has been studied using the most common technique of UV-Vis Spectrophotometric System and Quimioluminescence. In the study “*Investigation of iron (III) reduction and trace metal interferences in the determination of dissolved iron in seawater using flow injection with luminal chemiluminescence detection*”, kinetic experiments were conducted to examine the efficiency of reduction of inorganic Fe (III) with sulphite under different conditions and a rigorous study of the potential interference caused by other transition metals present in seawater was conducted (e.g. : [24]).

1.2 Importance of trace metal analysis

Trace metals are present in extremely small quantities (less than parts per million, ppm) which are essential for plants and animal existence. The most essential one are iron (Fe), magnesium (Mg), lithium (Li), zinc (Zn), copper (Cu), chromium (Cr), nickel (Ni), cobalt (Co), vanadium (V), arsenic (As), molybdenum (Mo) and selenium (Se). Knowledge of the concentration and distribution of trace metals in natural waters allows a better understanding of their biogeochemical behavior and cycling (e.g. : [3]). Among these ones of the most studied one is Iron. It is an element whose ions are found at trace levels in natural waters. Natural waters are non-homogeneous and rather complex systems, which normally consist of an aqueous phase, a gas phase and one or more solid phases.

This element, Fe, is the fourth most abundant element by weight in the earth's crust. The chemistry of aqueous iron primarily involves the ferrous (II) and ferric (III) oxidation states and it is of interest in water supplies, wastewaters, limnology, and oceanography (e.g. : [20]). Fe is an essential micronutrient in primary life production in the oceans, and is considered the limiting nutrient in water bodies. This metal in its oxidation state (III), Fe^{+3} is highly insoluble in water. The intake by microorganisms depends on the solubility of Fe ions. The dissolved ions of Fe depend of the balance between supplies sources and removal processes. When this balance is changed, the intake of Fe ions is affected. The need of Fe for the growth of phytoplankton has been demonstrated in studies of Enrichment Iron Experiment (IRONEX) under high nitrate (NO_3^-) concentration and low chlorophyll (e.g. : [11]). IRONEX studies are also known as iron fertilization, since it involves the intentional introduction of iron ions into oceans to stimulate the bloom of fitoplancton (e.g. : [7]). In 1993, the first IRONEX study were done in the Moss Landing Marine Laboratories at California state. Given the need for this ion in water, much effort have been put to determine the solubility of Fe ions as a function of temperature, salinity, pH and ionic strength of the medium.

Similarly, Copper (Cu) is a biologically important element at trace levels in water bodies. It exists in two oxidation states, Cu^{+2} and Cu^{+1} , but predominate in it oxidation state (II). Scientists have demonstrate that it is possible to find quantities of Cu^{+1} in natural waters due to the following reaction (e.g. : [15]):



Since Cu^{+2} is required to sustain aquatic life, it is of great interest to determine the amount of Cu ions present in the aquatic environment, due to the toxicity.

Natural waters composition is changing with the same intensity that increases global warming. Some climate models predict changes and serious consequences for the global climate system and water supply. For this reason, it is important to increase the understanding of redox processes of trace water bodies.

Previous studies of the kinetics of the redox process of Fe and Cu using Chemiluminescence and Spectrophotometry technique are reported in scientific literature [18, 19, 24]. These techniques are the most commonly used, but CV also is an appropriate technique for this type of analysis. CV is a highly sensitive technique that allows determining the nanomolar levels of Fe and Cu ions, as has been reported with other techniques. The major existing techniques for trace metal analyses are spectroscopic, in particular, graphite furnace atomic absorption spectroscopy (GF-AAS) and inductively coupled plasma mass spectroscopy (ICP-MS). Also, neutron activation analysis (NAA) has been widely used (e.g.: [10]). The advantage of NAA, GF-AAS and ICP-MS compared to voltammetric techniques is that they are applicable to a large number of elements. But, their major drawbacks are their much higher cost, and above all, the fact that they allow measurements of total concentration only (e.g.: [10]) and not the individual ions concentration in solution.

1.3 Advantage of using Cyclic Voltammetry technique for trace metal analysis

Although multiple chemical and spectroscopic analytical techniques exist for analysis of trace metal, CV is an important option for measuring trace metals. A fast-scan cyclic voltammetry has several advantages: rapid analysis in a times scale of seconds, a small

volume of sample is required (~5 to 10mL of solutions), provides quantification of metals ions, simultaneous determination of several analytes (electroactive species), a large number of useful solvents and electrolytes, and the ability to determine kinetic parameters. The CV technique also discriminate the elements with different oxidation state (such as Cu^{+2} and Cu^{+1}).

Another advantage is its relative low cost. CV instrumentation varies from \$3,000 to \$22,000. When compare CV price with other instrumentation such as High-performance liquid chromatography (HPLC), Inductively Coupled Plasma - Mass Spectrometry (ICP-MS) and Graphite Furnace Atomic Absorption (GFAA)), it is much more economic and cost effective. Refer to table 1 to compare prices.

Table 1. List of price of four analytical techniques used for trace metal analysis.

Techniques	Model	Manufacture/Distributors	Price (USA dollars)
Cyclic Voltammetry	EC Epsilon	BASi	\$11,300
HPLC	1200 Infinity	Agilent Technologies	\$60,000
	1100 Infinity	Agilent Technologies	\$150,000
ICP-Mass Spectroscopy	7500	Agilent Technologies	\$150,000
GFAA	3310	Perkin Elmer	\$60,000

Chapter II: Literature Review

The Cu and Fe ions concentration in seawater has been studied using mainly chemistry, photochemistry and geochemistry methods. Do to the importance of the redox process of these metals with O_2 and H_2O_2 for the global warming, many laboratories had also put effort to study these interactions with these technique.

In 1980, Windsor Sung and James J. Morgan (e.g.: [27]) studied spectroscopically the “*Kinetics and Product of Ferrous Iron Oxygenation in Aqueous Systems*”. The purpose of their work was to study the effect of ionic media, alkalinity, and temperature on the kinetics of ferrous iron oxygenation. They were also interested in determining the product of oxygenation. Ferrous iron concentration was determined spectrophotometrically complexes with 1,10-phenanthroline, using fluoride as a masking agent for ferric iron. Beer's law was obeyed with ferrous iron concentration as high as 7 mg/L (equivalent of 0.125 μM). Ferric iron was used as a blank with concentration as high as 2500 mg/L (0.04476 μM). The molar absorptivity at 510 nm was determined to be 10,500 $M^{-1} cm^{-1}$ with accuracy better than 1%.

W. Davison and G. Seed (e.g.: [28]) studied “*The kinetics of the oxidation of ferrous iron in synthetic and natural waters*”. The oxidation rate of ferrous iron during the seasonally anoxic lake was measured on 39 occasions with respect to depth and time. Minimal sample disturbance was done when oxygen was introduced to initiate the reaction. The obtained data were consistent with the simple rate law for homogeneous chemical kinetics previously established for synthetic solutions. The rate constant for the oxidation reaction in the lake water was indistinguishable from that measured in

synthetic samples. Changes in microbial population, particulate or soluble components (including iron and manganese) in water do not appear to influence the rate constant. Analysis of the errors inherent in the kinetic measurements showed that the estimation of pH was the major source of inaccuracy and that values of the rate constant determined by different workers could easily differ by a factor of six. The present data, together with a comprehensive survey of the literature, are used to suggest a 'universal' rate constant of $ca. 2 \times 10^{13} \text{ M}^{-2} \text{ atm}^{-1} \text{ min}^{-1}$ (range $1.5\text{--}3 \times 10^{13}$) in the rate law

$$-\frac{d[FeII]}{dt} = k[FeII]pO_2(OH^-)^2 \quad (1)$$

for natural freshwaters in the pH range 6.5–7.4. Discrepancies in the effects of ionic strength and interfering substances reported in the literature are highlighted. Generally substances have only been found to interfere at concentrations which far exceed those in most natural waters.

In the Division of Marine and Atmospheric Chemistry at Rosenstiel School of Marine and Atmospheric Science (RSMAS) of the University of Miami, the investigators Frank J. Millero and coworkers are interested in the application of physical chemical principles for the analysis of natural waters. They attempt to understand how ionic interactions affect the thermodynamics and kinetics of processes occurring in the oceans. Also, they use ionic interaction models to estimate the activity and speciation of ions in natural waters of known composition. Their natural water samples are obtained from Southern Ocean, North Atlantic, Indian Ocean, Bahamas Banks and Florida Bay.

In 1984, Millero and co-workers (e.g.: [29]) investigated “*The effect of ionic interactions on the oxidation of metals in natural waters*”. His research group studied specifically the ionic interactions of the major components of natural waters on the oxidation of Cu (I) and Fe (II). The various ion pairs of these metals have been shown to have different rates of oxidation. For Fe (II), the chloride (Cl⁻) and sulfate (SO₄⁻²) ion are not easily oxidized. This measurement decrease in a fixed pH in chloride and sulfate solutions agrees very well with the values predicted. The effect of pH (6 to 8) on the oxidation of Fe (II) to Fe (III) in water and seawater have been shown to follow the rate equation:

$$-\frac{d \ln[Fe(II)]}{dt} = \frac{k_1 \beta_1 \alpha_{Fe}}{[H^+]} + \frac{k_2 \beta_2 \alpha_{Fe}}{[H^+]^2} \quad (2)$$

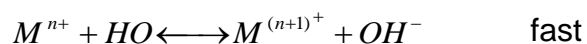
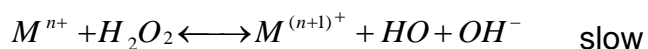
where k_1 and k_2 are the pseudo first order rate constants, β_1 and β_2 are the hydrolysis constants for Fe(OH)⁺ and Fe(OH)⁰. The value of α_{Fe} is the fraction of free Fe²⁺. The value of k_1 (2.0 ± 0.5 min⁻¹) in water and seawater are similar within experimental error. The value of k_2 (1.2 × 10⁵ min⁻¹) in seawater is 28% of its value in water in reasonable agreement with predictions using an ion pairing model.

For the oxidation of Cu(I) a rate equation of the form:

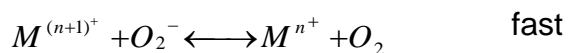
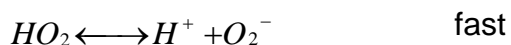
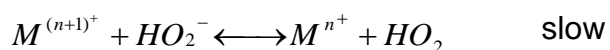
$$-\frac{d \ln[Cu(I)]}{dt} = k_0 \alpha_{Cu} + k_1 \beta_1 \alpha_{Cu} [Cl] \quad (3)$$

was found, where k_0 (14.1 sec⁻¹) and k_1 (3.9 sec⁻¹) are the pseudo first order rate constants for the oxidation of Cu⁺ and CuCl⁰, β_1 is the formation constant for CuCl⁰ and α_{Cu} is the fraction of free Cu⁺. Thus, unlike the results for Fe(II), Cu(I) chloride complexes have measurable rates of oxidation.

The interaction of peroxide with Fe and Cu was studied by J. W. Moffett and R. G. Zika (e.g.: [12]). In 1987, these investigators studied the “*Reaction kinetics of hydrogen peroxide with copper and iron in seawater*”. The oxidation of Fe (II) and Cu (I) and the reduction of Fe (III) and Cu (II) by hydrogen peroxide in seawater have been studied to understand their mechanisms and probable significance in the upper marine water column. At 10^{-7} M H_2O_2 , a level commonly found in surface seawater, reaction with H_2O_2 is the dominant oxidation pathway for Fe (II). A generalized mechanism for Cu (I) and Fe(II) oxidation has been proposed by earlier workers (e.g.: [31,32]):



And for Cu (II) and Fe (III) reduction, the following mechanism has been proposed (e.g: [32]):



Reduction of Fe (III) by peroxide was not observed in the pH range 7-8. Reduction of Cu(II) and oxidation of Cu (I) by H_2O_2 , contribute to a dynamic redox cycling of that element in the upper water column. The rate constants for Fe (II) and Cu (I) were $5 \times 10^{-3} \text{ s}^{-1}$ and $1 \times 10^{-5} \text{ s}^{-1}$, respectively. Calculations based on these data indicate that Cu (I) oxidation and Fe (II) oxidation by H_2O_2 are at least as important as nitrite photolysis as a source of OH radicals in the ocean.

The peroxide formation in natural water was analyzed by W. J. Copper and R. G. Zika in 1988 (e.g.: [32]). They studied the “*Photochemical formation of hydrogen peroxide in natural waters exposed to sunlight*”. Hydrogen peroxide is formed in natural waters exposed to sunlight. The rate at which H_2O_2 accumulates is related to the concentration of organic substances absorbing light of $>295\text{ nm}$ in these waters. The photochemical accumulation rate of H_2O_2 in sunlight has been measured for several surface waters and groundwater, and was found to be in the range of 2.7×10^{-7} to $48 \times 10^{-7}\text{ mol L}^{-1}$, in waters containing 0.53 to 18 mg L^{-1} dissolved organic carbon, respectively. These rates were determined in midday sunlight with an intensity light power of 0.4 W m^{-2} ($295\text{-}385\text{ nm}$), latitude 24.3° N . Apparent quantum yields of H_2O_2 have been determined for natural waters at different wavelengths. These quantum yields decreased with increasing wavelength, from 10^{-3} in the near-ultraviolet to 10^{-6} in the visible spectral range. The quantum yields have been used in a photochemical model to calculate H_2O_2 accumulation rates of natural water samples. Model calculations agree with H_2O_2 accumulation rates obtained from exposing three different water samples to sunlight.

In 1992, the effect of ionic interaction on “*The rates of reduction of Cu(II) with H_2O_2 in aqueous solutions*” was studied by F. J. Millero, R. L. Johnson, C. A. Vega, V. K. Sharma, and S. Sotolongo (e.g.: [7]). They investigate the rates of reduction of Cu (II) with H_2O_2 in NaCl and NaBr solutions and mixtures with NaClO_4 as a function of pH (6 to 9), temperature (5 to 45°C) and ionic composition (0.1 to 6.0M). The effect on pH on the rate was found to be independent of the temperature and ionic composition. The rates increased as a function of $[\text{H}^+]$ raised to the power of 1.3 to 1.6. Their speciation

calculation indicated that this pH dependence can be attributed to $\text{Cu}(\text{OH})_2$, being the reactive species. The rate constant in NaCl and NaBr and mixtures with NaClO_4 were independent of ionic strength, but proportional to the halide concentration raised to the power of 2.0 (0.2 to 2.6M). These results can be attributed to $\text{Cu}(\text{OH})_2\text{Cl}_2^{-2}$ being the reactive species to the reduction with H_2O_2 . They found that the Cu (I) halide complexes formed from the reduction were not easily oxidized with O_2 or H_2O_2 . The faster rate in Br⁻ solution forming stronger complexes with Cu^+ was demonstrated in their investigation.

In 2001, Carmen. A. Ribera Gonzalez mentored by C. Vega Olivencia(e.g.: [33]) studied the concentration of Fe^{+2} present in ocean water and also not treated industrial water using CV technique. This study was entitled “*Electrochemistry studied of the interaction of Iron (II) with peroxide in natural and industrial waters*”. The samples were collected from the northwest region of Puerto Rico. In this area there are localized several industries. The aim of her research was to determine the concentration of Fe, and calculates the kinetic for the oxidation of Fe^{+2} with H_2O_2 . The instrument used was a BASCV50W connected to a C2-Cell Stand with a three electrode arrangement: Platinum working electrode (PWE), Ag/AgCl as reference electrode, and a platinum wire as auxiliary electrode. Detail of the instrumentation use in these in our day laboratory will be presented in Chapter III of this thesis report. Before polishing process, the PWE required a pretreatment with 5% w/v nitric acid to eliminate metallic residues adsorbed in the electrode surface.

The potential window used was from -0.40V to -0.80V, which allowed to examine the oxidation current of Fe^{+2} to Fe^{+3} at a sweep rate of 10mV/s. Even though a slow sweeping rate it was possible to observe an intense oxidation current generated at the WE versus the platinum auxiliary electrode.

The Fe ion concentration in the samples were determined using the standard addition method. In this method, a sample of unknown concentration ions is analyzed when a set of samples of known concentration. For this particular work, the water samples were analyzed making consecutive addition of $2.0 \times 10^{-3} \text{M}$ $\text{Fe}(\text{NH}_4)_2(\text{SO}_4)$ solution. Five increments of 50 μL of standard solution were added, and at every addition a new voltammogram was taken. As the result of this investigation the Fe^{+2} concentrations found in ocean water was $3.1 \times 10^{-4} \text{M}$, and $4.4 \times 10^{-4} \text{M}$ for the nontreated industrial water.

C. Ribera also did a kinetic studies for the oxidation of Fe^{+2} to Fe^{+3} using H_2O_2 , as the oxidant agent, addition to the reaction electroanalytical cell. The oxidation current peak ($i_{p,a}$) was decreasing as function of time as five consecutive cycles were swept. The $i_{p,a}$ decreases due to the elimination from the bulk of the solution. The concentration of Fe^{+2} as H_2O_2 oxidized it, and this decrease is monitored at the WE surface. The rate of the oxidation of $\text{Fe}^{+2} + \text{H}_2\text{O}_2 \rightarrow \text{Fe}^{+3} + \text{OH} + \text{OH}^-$ was calculated from the slope of the $\Delta i_{p,a}$ vs. time (sec.) curve. In order to determine the kinetic constant $\left(K = \frac{\partial[\text{Fe}^{+2}]}{\partial t} \right)$ it is necessary built a calibration curve ($i_{p,a} \propto [\text{Fe}^{+2}]$). The $i_{p,a}$ of the unknown concentration can be estimated at every cycle, and the slope of the curve represent (K).

A window from a range of -0.50V to -0.80V was used this time in five potential consecutive sweep were trace. This potential window allows the calculation of the rate constant. A constant of 1.5×10^{-3} gFe/s was found. This value compares with the reported values using spectroscopic techniques. Table 2 summarize these values. In this investigation using the cyclic voltammetry technique detection limits of the order 10^{-7} M were found, allowing this technique to be considered an easy, fast and feasible alternative to determine concentrations in the part per billion (ppb) range.

Table2. Rate constant for Fe^{+2} and Cu^{+} oxidation with H_2O_2 and O_2 in seawater (e.g. : [12]).

Rate Constant	Reference
$\text{Fe}^{+2} + \text{H}_2\text{O}_2 \rightarrow \text{Fe}^{+3} + \text{OH} + \text{OH}^-$	
$k = 5.0 \times 10^{-3} \text{ s}^{-1}$	Moffett and Zika
$\text{Fe}^{+2} + \text{O}_2 \rightarrow \text{Fe}^{+3} + \text{O}_2^-$	
$k = 2.2 \times 10^{-3} \text{ s}^{-1}$	Millero
$k = 6.7 \times 10^{-4} \text{ s}^{-1}$	Waite and Morel
$k = 5.8 \times 10^{-4} \text{ s}^{-1}$	Murray and Gill
$k = 7.6 \times 10^{-4} \text{ s}^{-1}$	Kester
$\text{Cu}^{+} + \text{O}_2 \rightarrow \text{Cu}^{+2} + \text{O}_2^-$	
$k = 7.8 \times 10^{-4} \text{ s}^{-1}$	Moffett and Zika
$\text{Cu}^{+} + \text{H}_2\text{O}_2 \rightarrow \text{Cu}^{+2} + \text{OH} + \text{OH}^-$	
$k = 1 \times 10^{-5} \text{ s}^{-1}$	Moffett and Zika
$[\text{O}_2] = 2.1 \times 10^{-4} \text{ M}, [\text{H}_2\text{O}_2] = 1 \times 10^{-7} \text{ M}, T = 25 \text{ }^\circ\text{C}, \text{pH } 8.0.$	

Recently, Stripping Voltammetry (e.g.: [5]) has been the electrochemistry technique mostly used for trace metal analysis among other technique. The Stripping Voltammetry technique consist of a preconcentration step, at an appropriate voltage, followed by the stripping step, thereby, enhancing sensitivity and selectivity (e.g.: [4]). During the preconcentration step, the trace metal of interest is collected in the working electrode, and during the stripping step the collected metal is oxidized or reduced back into solution (e.g. : [5]). This technique allow to determine concentrations in the range of 10^{-6} to 10^{-12} . Table 3 summarize the major voltammetric techniques used for trace metal analysis and their typical concentration ranges.

Table 3. Major voltammetric techniques used for trace-metal analysis and their typical concentration ranges. v = Potential scan rate (mV/s); DP = Pulse amplitude; f = Frequency; t_d = Preconcentration time; i_p = Peak current; E_p = Peak potential (e.g. : [8]).

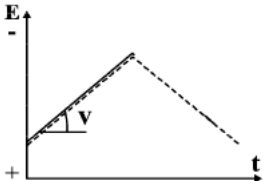
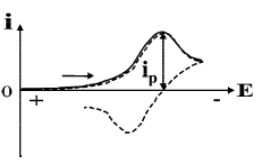
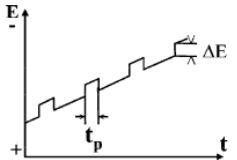
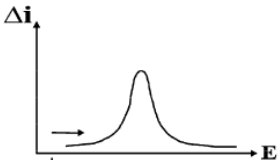
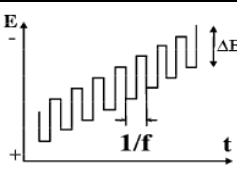
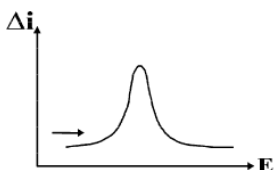
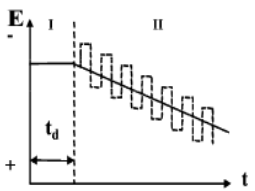
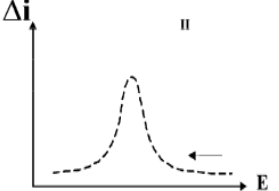
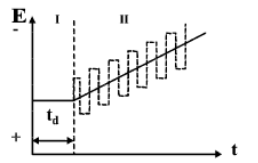
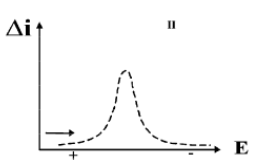
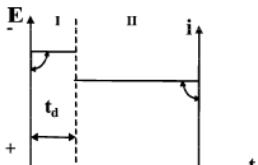
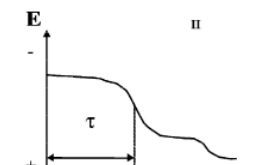
Technique	Imposed function	Recorded function	Conc. Range (mole L)
Linear sweep voltammetry (LSV) (cyclic voltammetry dotted line)			$10^{-2} - 10^{-6}$
Differential pulse voltammetry (DPV)			$10^{-4} - 10^{-7}$
Square wave voltammetry (SWV)			$10^{-4} - 10^{-8}$
Anodic stripping voltammetry (ASV) with linear scan (full line) or modulation (e.g. DP → DPASV or SW → SWASV; dotted line)			$10^{-6} - 10^{-11}$

Table continued in the next page

Table 3.(Continued) Major voltammetric techniques used for trace-metal analysis and their typical concentration ranges. v = Potential scan rate (mV/s); DP = Pulse amplitude; f = Frequency; t_d = Preconcentration time; i_p = Peak current; E_p = Peak potential (e.g. : [8]).

Technique	Imposed function	Recorded function	Conc. Range (mole L)
Adsorptive stripping voltammetry (AdSV) (with or without modulation)			$10^{-6} - 10^{-12}$
Stripping chronopotentiometry (SCP)			$10^{-5} - 10^{-9}$

At this moment little is known, and very few scientific publications have been reported for trace metal analysis using Cyclic Voltammetry. For the last decade, in our electroanalytical research laboratory at the University of Puerto Rico, Mayaguez Campus, much effort has been conducted to study the kinetic and redox process of Fe and Cu ions in natural waters using CV technique. In our study the concentration of Fe ion and Cu ion present in natural waters are determine using Cyclic Voltammetry. Also the kinetic rate for the oxidation of Fe(II) and Cu (I) with H_2O_2 has been analyzed.

Chapter III: Instrumentation

3.1 Cyclic Voltammetry Instrumentation

The basic components of a modern electrochemical system for voltammetry are a potentiostat, the electrochemical cell and a computer. These components are shown in figure 1. The potentiostat applied the desired potential and monitors the current response. A three electrode system connected to a potentiostat is used for CV experiments. Why do it is needed three electrodes for CV? The use of two electrodes, such as the one uses for pH measurement, does not permit to control the external applied potential to the system. Therefore, a precise control is required and it can be achieved using a potentiostat and a three electrode system.



Figure 1. EC-Epsilon potentiostat connected to a BASi C-3 Cell Stand (e.g. : [2])

3.1.1 Electrochemical workstation

The electrodes required are the working, reference and auxiliary electrode. The cell used is a Bionalytical System, C-3 glass vial with a fitted top that accommodate the three electrode array, and a tube for deoxygenation of the solution studied by bubbling

with a stream of high-purity nitrogen gas. In this system, the potential of the working electrode is controlled relative to a reference electrode, and the current passes between the working electrode and the auxiliary electrode (e.g.: []). Figure 2 show a representation of the BASi C-3 Cell Stand with its components; vial, electrode and top.



Figure 2. BASi C-3 Cell Stand

It is important to understand the role of each electrode. They are electronic conductors that influence the transport of charges across interfaces between the electrode/electrolyte interphase. When a potential is applied to the working electrode, electrons are moved to the electrode surface. The most used WE materials are solid metal, liquid metal, carbon and semiconductors. For the analysis of trace metals the WE used is a BASi MF-2012 Glassy Carbon (GCE). The electrode is manufactured in a solvent-resistant Chlorotrifluoroethylene (CTFE) plastic body of 7.5 cm length and 6 mm outer diameter which is embedded with a highly polished disk of glassy carbon. The electrode disk diameter is 3.0 mm. The reference electrode is typically a BASi RE-5B Silver/Silver Chloride electrode with a flexible connector. It has a 6 mm outside diameter glass body, 7.5 cm long and uses a porous junction made from Vycor, a glass with high temperature and thermal shock resistance. The auxiliary electrode used is a BASi MW-1032 platinum wire of 7.5 cm and 0.5mm diameter. The platinum wire provides a surface for a redox reaction to balance the half reaction occurring at the surface of the working electrode (e.g. : [2]). Figure 3 Shows a typical diagram of the three electrodes; a) working electrode, b) reference electrode and c) auxiliary electrode.

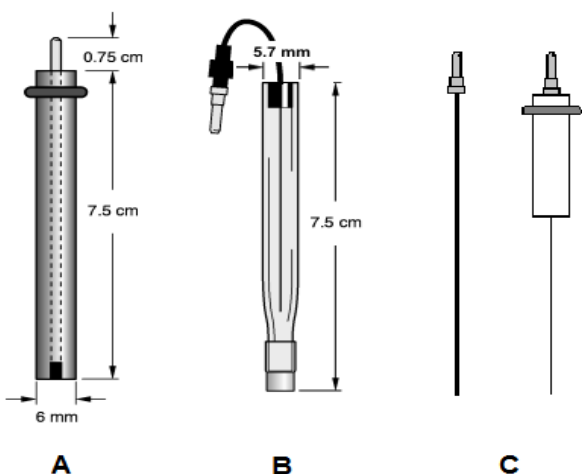


Figure 3. **a)** Standard BASi working electrode, **b)** Silver/Silver Chloride Reference electrode RE-5B (Ag/AgCl) and **c)** Auxiliary electrode (e.g. : [2]).

3. 2 Basic Principles of Cyclic Voltammetry

CV is an effective and versatile electroanalytical technique that allow mechanistic studies of redox systems. It is a potential-controlled reversal electrochemical technique. A cyclic potential sweep is imposed on an electrode, and the current response is measured. Specifically, the potential is applied between the reference electrode and the working electrode and the current is measured between the working electrode and the counter electrode. Commonly a triangular potential wave, such as the one shown in figure 4, is applied to a $1.0 \times 10^{-3}\text{M}$ solution of Cu^{+2} in 0.1M NaCl electrolyte supporting solution. In figure 1, the potential is first varied linearly from a positive voltage ($+0.35\text{V}$) to a negative voltage (-0.15V) versus an Silver/Silver Chloride (Ag/AgCl) electrode used as a reference electrode. At this negative potential the scan direction is reversed, and the potential is returned to its original value completing the voltage cycle. A scan in the direction of more negative potential is called a forward scan, while the one in the opposite direction is called a reverse scan. Sometimes, one cycle is sufficient to perform the experiment, while in other instances, a large number of cycles is required. For each cycle the potential (E) is vary linearly in one direction and then in the reverse direction.

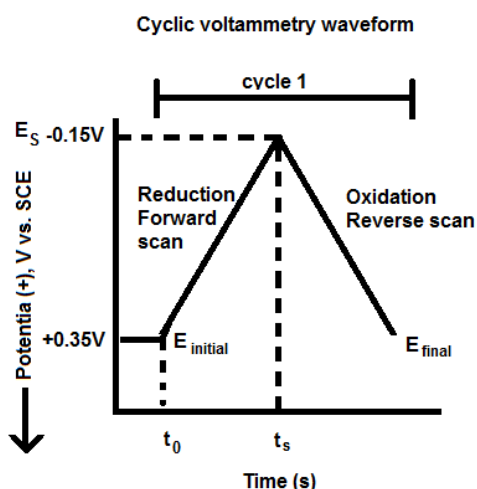


Figure 4. Triangular potential waveform for one cycle in a CV experiment.

A cyclic voltammogram is a current-potential curve plotted where the dependent variable is the current (μA) obtained versus potential (mV) scan as the independent variable. Figure (5-A) show a typical cyclic voltammogram for an electroactive species. There are a variety of voltammograms shapes (fig.5-B) that can be obtained and their interpretation helps to understand redox processes occurring in solution. Analysis of the voltammogram provides information about the thermodynamic and kinetics of electron transfers at the electrode surface interface.

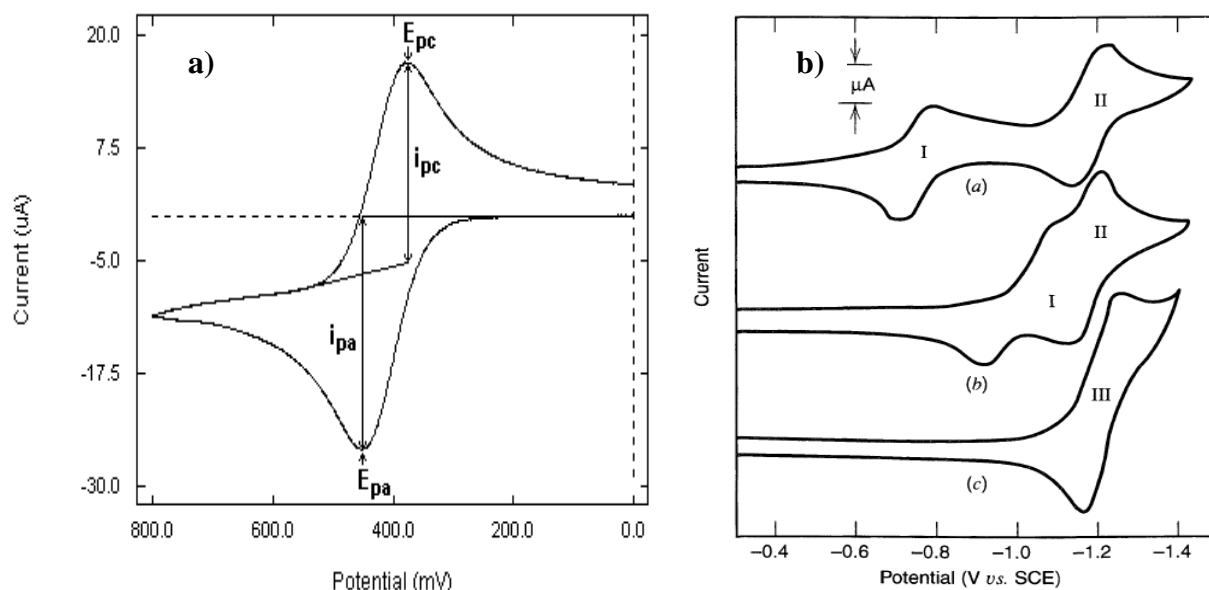


Figure 5: **a)** Typical cyclic voltammogram with polarographic scale using software for BAS5-Epsilon, **b)** variety of cyclic voltammograms.

Important parameters in a cyclic voltammogram are the peak potentials (E_p) and peak currents (i_p). Scanning in the negative direction, at sufficiently negative potential, a reduction peak (or cathodic peak) appears corresponding to the reduction of electroactive specie in solution. The peak area is proportional to the amount of electrons crossing the interface. If the redox couple is reversible then when the applied potential is reversed, in the positive direction, it will reach the potential that will reoxidize the

product formed in the first reduction reaction, and produce a current of reverse polarity from the forward scan. This means that an oxidation process occurs and the oxidation peak (or anodic peak) appears. Analysis of the current response provides information about the thermodynamics of reactions and kinetics of electron transfer at the electrode-electrolyte interface. The measured current is a function of the applied potential and the concentration of the electroactive species. The proper equilibrium ratio at a given potential is determined by the Nernst Equation:

$$E = E^{0'} - \frac{RT}{nF} \ln \left(\frac{[R]}{[O]} \right)_{x=0} \quad (4)$$

Where O is the oxidized form, R is the reduced form and $E^{0'}$ is the formal potential at the surface of the electrode ($x=0$).

3.2.1 Factors affecting the electrode reaction rate and current

Consider an overall electrode reaction, $O + ne \leftrightarrow R$, composed of a series of steps that cause the conversion of the dissolved oxidized species, O, to a reduced form, R, also present in solution (Figure 6). In general the current is governed by the rates of processes such as (e.g.: [1]):

1. Mass transfer (e.g., of O from the bulk solution to the electrode surface).
2. Electron transfer at the electrode surface.
3. Chemical reactions preceding or following the electrode surface. These might be homogeneous processes (e.g., protonation or dimerization) or heterogeneous ones (e.g., catalytic decomposition) on the electrode surface.
4. Other surface reaction, such as adsorption, desorption, or crystallization (electrodeposition).

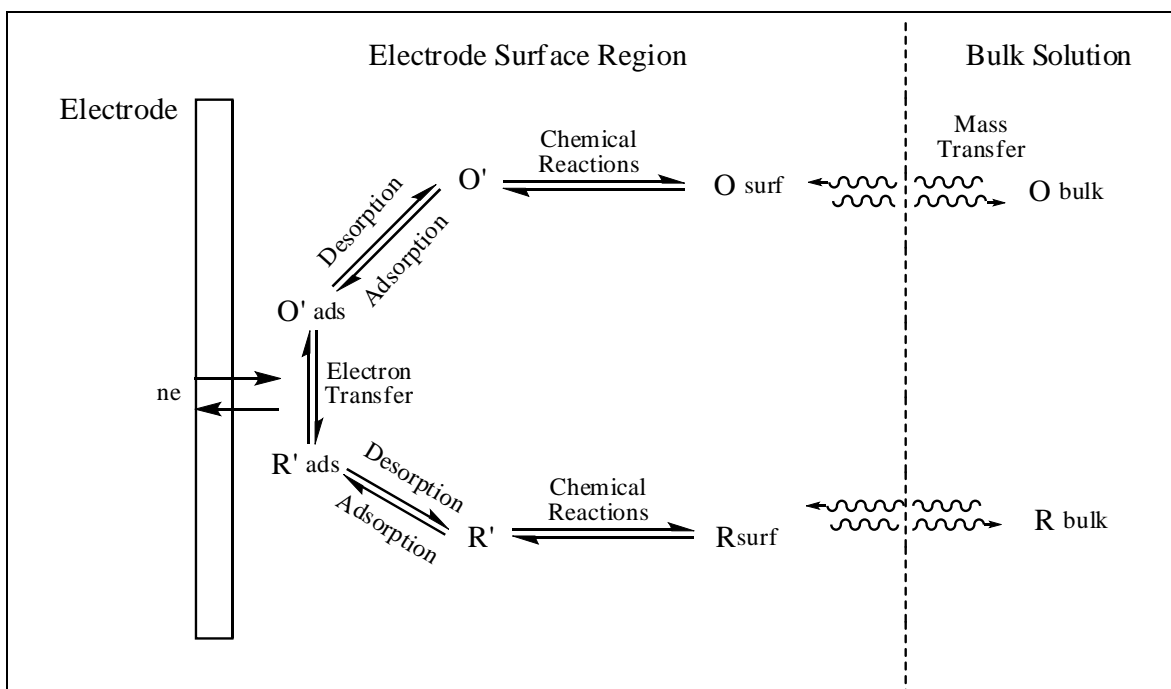


Figure 6. General pathway of a general electrode reaction of oxidized (O) and reduced (R) electroactive species.

In order to make possible the electrode reaction, the electroactive specie has to move from the bulk solution to the electrode-solution interface. As mentioned, the rate of transport to the surface can also effect or even dominate the overall reaction rate and three different forms of mass transport that can influence electrolysis reactions; Convection, Migration and Diffusion. Convection is a mode of mass transport where the electroactive specie is moved by the influence of density gradient, laminar flow, turbulent flow and agitation. Migration refers to the movement of an electroactive species under the influence of an electric field. Diffusion is the movement of an electroactive species under the influence of a gradient of chemical potential, such as a concentration gradient. In the electrolysis reaction the electroactive specie has to transport by diffusion. The use of an electrolyte solution, an electrochemically inert salt, such as NaCl at a high concentration (0.1 M), favors the diffusion to be the only form of mass transport.

The rate of movement of material by diffusion can be predicted mathematically by the Fick first law equation (e.g.: [1]):

$$J_o = -D_o \frac{\partial c_o}{\partial x} \quad (5)$$

This equation relates the diffusional flux J_o (mol/m²s) to the concentration gradient and the diffusion coefficient, D_o (m²s⁻¹). J_o measures the amount of substance that will flow through a small area during a small time interval. The negative sign compensates for the fact that the electroactive species move from a high concentration toward a lower concentration.

The transference of the electron occurs via a quantum mechanical tunneling between the electrode and reactant close to the electrode. Typical surface tunnelling distances are less than 2 nm. Finally, the product (R) moves away from the electrode-solution interface allowing fresh reactant to move toward the surface. A simple example of an electrode reaction is shown in figure 7. In this figure, the reactant Fe^{+3} moves to the interface electrode-solution where it undergoes a one-electron reduction to form Fe^{+2} .

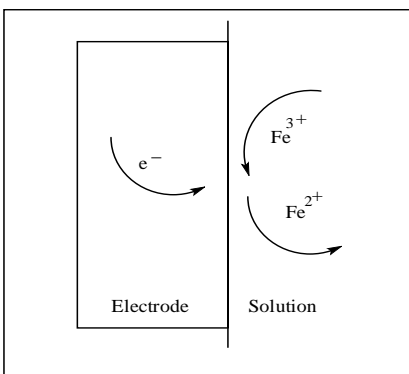
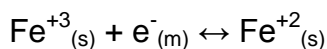


Figure 7. A single electrode reaction.

3.2.2 Reversible electrochemical reaction

Among electroactive species, there are three possible type of electrochemical behavior for the electrocatalyzed redox processes: reversible, quasi-reversible or irreversible. Reversible means that the reaction is fast enough to maintain the concentration of the oxidized and reduced forms in equilibrium with each other at the electrode surface.

For a reversible process at 25°C, $\Delta E_p = |E_{cathodic} - E_{anodic}|$ lies within the range of 60 to 90mV. Example of a reversible process is shown in figure 8, where $E_c = 72\text{mV}$ and $E_a = 162\text{mV}$ and $\Delta E_p = |72\text{mV} - 162\text{mV}| = 90\text{mV}$. Also, the peak currents ratio (i_{pc}/i_{pa}) passed is near unity.

$$1 = \frac{i_{pa}}{i_{pc}} \quad (6)$$

Therefore, if the ratio in equation 1 is less than or greater than 1, the process is semi-reversible.

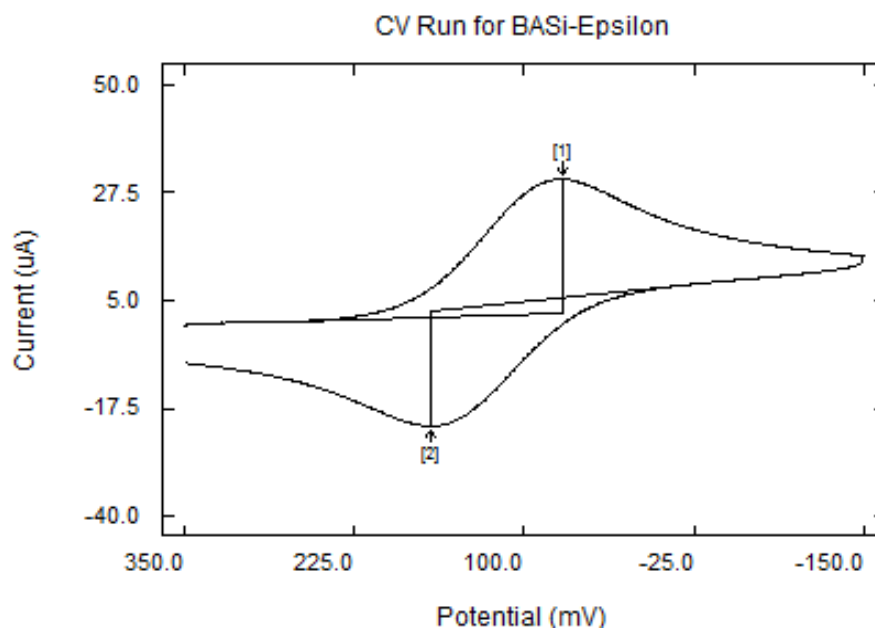


Figure 8. Voltammogram of 1mM Cu^{+2} at a scan rate of 500mV/s and a sensitivity of $100\mu\text{AV}^{-1}$ with Ag/AgCl as the reference electrode and polarographic scale using software for BASi-Epsilon

For an irreversible process, ΔE is greater than 90mV and its electron transfer is so slow that only one process occurs, reduction or oxidation. An example of a cyclic voltammogram corresponding to an irreversible process is shown in figure 9, where the electroactive species is reduced when scanning in the negative direction. However, no anodic peak is observed under the influence of positive potentials at the reversed direction.

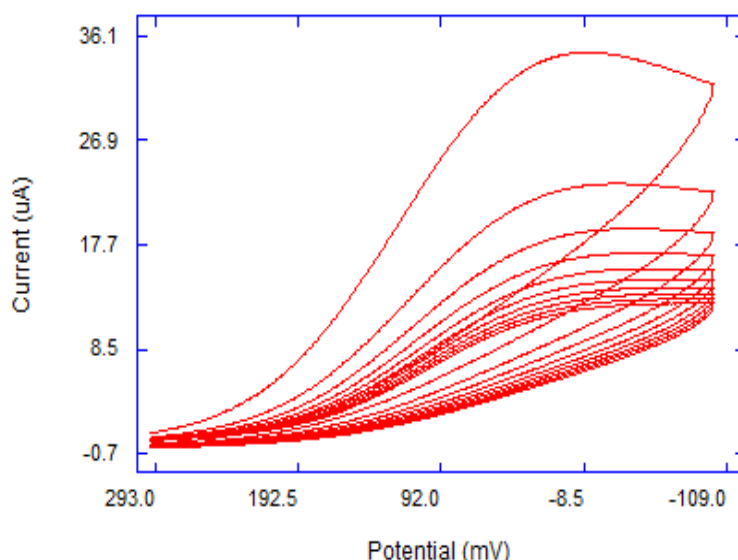


Figure 9. Voltammogram of an irreversible process.

3.2.3 Nernst Equation

The Nernst equation describes the fundamental relationship between the potential applied to an electrode and the concentration of the redox species at the electrode surface (e.g.: [2]). If an electrode is at equilibrium with the solution in which it is immersed, the electrode will have a potential, invariant with time, which is thermodynamically related to the composition of the solution. In solution, species O is

capable of being reduced to R at the electrode by the following reversible electrochemical reaction.



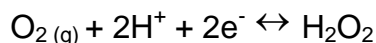
This equation relates the potential, E, which is applied to the electrode and the concentrations of species O and R at the electrode surface:

$$E = E^{0'} - \frac{RT}{nF} \ln \left(\frac{[R]}{[O]} \right)_{x=0} \quad (7)$$

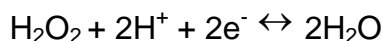
Where, E is the potential applied to electrode, $E^{0'}$ is the formal reduction potential of the couple vs. reference electrode, n is the number of electrons, [R] and [O] are the surface concentration of species R and O, respectively. But, the Nernst equation describes the relationship for reversible equations. In other words, those are systems for which the electrode reaction in the $O + ne^- \leftrightarrow R$ is rapid in both directions.

3.2.4 Oxygen reduction interference

Dissolved oxygen in solution is easily reduced on the surface of an electrode. Two typical peaks are observed when an aqueous solution saturated with air (without a degas processes) is analyzed by CV technique. The first peak is the result of the oxygen reduction to hydrogen peroxide (e.g.: [25]):



The second peak corresponds to the reduction of the hydrogen peroxide previously formed.



The presence of oxygen may interfere in the determination of other species that overlap with these processes. The degasification of the solution for few minutes with an inert gas (such as ultrapure N₂) eliminates the interference of oxygen peaks (e.g.: [25]).

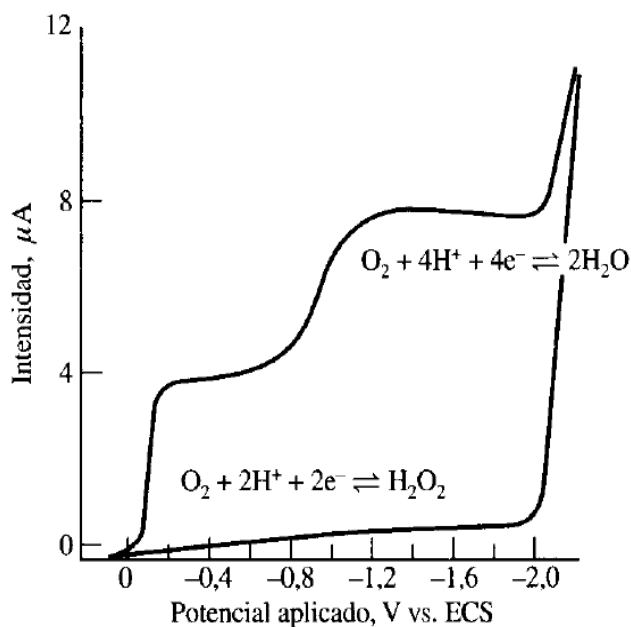


Figure 10. Voltammogram of the oxygen reduction in a solution saturated with air vs. Saturated Calomel Electrode (ECS) as reference electrode (e.g.: [25]).

3.2.5 Calculating the number of electrons involved in the bulk redox reaction in the electrochemical experiments.

The number of electrons transferred in a reversible reduction process, when R is initially absent, can be obtained through the following equation:

$$E_{pa} = E_{1/2} + \frac{RT}{nF} \log \left(\frac{i_l - i}{i} \right) \quad (8)$$

$$E_{pa} = E_{1/2} - \left(\frac{0.0592}{n} \right) \log \left(\frac{i_l - i}{i} \right) \quad (9)$$

Where E_{pa} refer to the anodic peak potential, $E_{1/2}$ is the half-wave potential for the reduction process (fig. 11-A) and it is independent of the substrate concentration. i_l is the limiting current or maximum current required to reduce the electroactive species at the surface electrode, i is the measured current and n is the number of electrons transferred during the oxidation process. The gas constant, R , is $8.314 \text{ Jmol}^{-1}\text{K}^{-1}$ and Faraday constant is $96,485 \text{ Cmol}^{-1}$ and for $T=298.16 \text{ K}$, $\frac{RT}{F} = 0.0596$

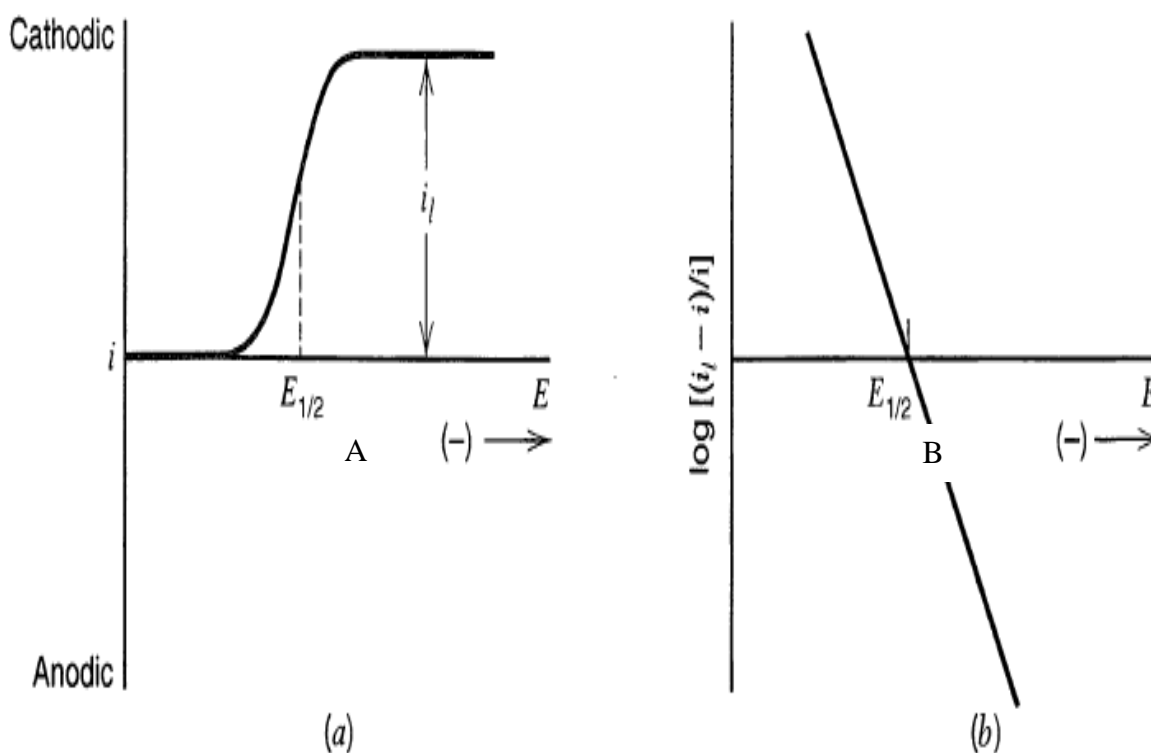


Figure 11. **a)** Current-potential curve for a Nernstian reaction involving two soluble species with only oxidant present initially. **b)** $\log[(i_l - i)/i]$ vs. E for a system (e.g.: [1]).

For a reversible process, it is expected that the corresponding E_{pa} vs. $\left(\frac{i_l - i}{i}\right)$ plot fits into linear regression with slope $\left(\frac{2.3RT}{nF}\right)$ (or 59.1/n, mV at 25°C). Alternatively (figure 11-B), $\log\left(\frac{i_l - i}{i}\right)$ vs. E is linear with slope of $\left(\frac{nF}{2.3RT}\right)$ (or $n/59.1$ mV⁻¹ at 25°C) and has an E-intercept of $E_{1/2}$. As result, the number of electron is obtained by the following equation:

$$n = -\left(\frac{2.3mRT}{F}\right) \quad (10)$$

3.3 Standard Addition Method in the Electrochemical Experiments

The method of standard addition is used to determine concentration of an analyte in an unknown sample by comparison to a set of samples of known concentration, similar to using a calibration curve. The reason for using the standard additions method is that the matrix may contain other components that interfere with the analyte signal, causing inaccuracy in the determined concentration. A typical procedure involves preparing several solutions containing the same amount of unknown, but different amounts of standard. The idea of this procedure is that the total concentration of the analyte is the combination of the unknown and the standard, and that the total concentration varies linearly. If the signal response is linear in this concentration range, then a plot similar to what is shown in figure 12 is generated.

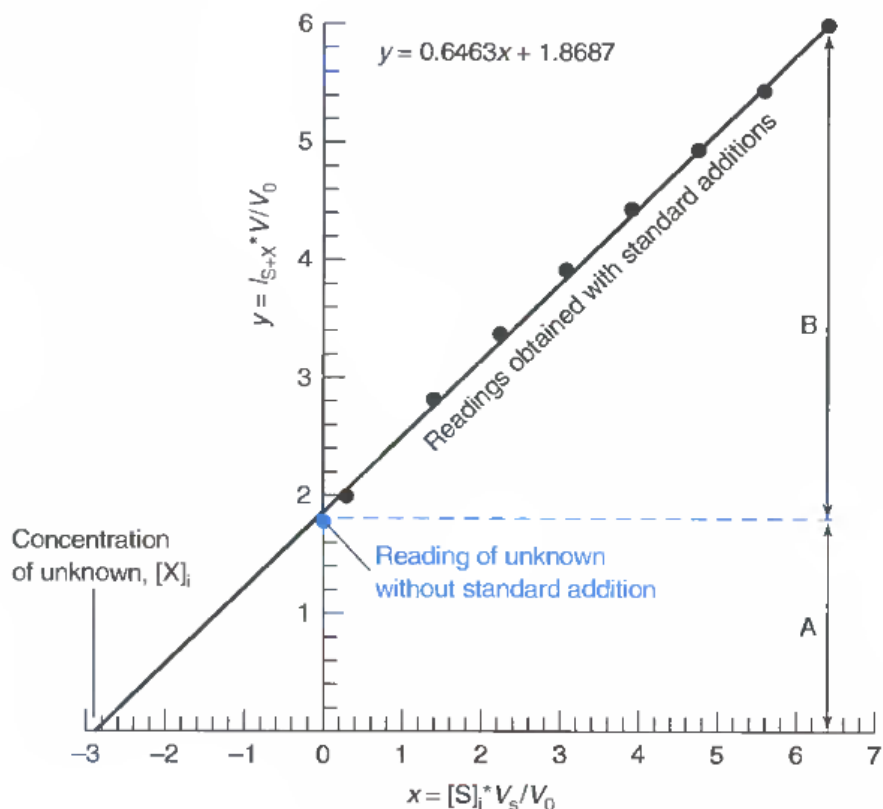


Figure 12. A standard addition plot

Consider a standard addition in which a sample with unknown initial concentration of analyte $[X]_i$ gives a signal intensity I_x . Then a known concentration of standard, S , is added to an aliquot of the sample and a signal I_{s+x} is observed for this second solution. Addition of standard to the unknown changes the concentration of the original analyte because of dilution. Let's call the diluted concentration of analyte $[X]_f$, where "f" stands for "final." We designate the concentration of standard in the final solution as $[S]_f$ (Bear in mind that the chemical species X and S are the same.)

Signal is directly proportional to analyte concentration, so

$$\frac{\text{Concentration Analyte in Initial Solution}}{\text{Concentration Analyte} + \text{Standard Final Solution}} = \frac{\text{Signal Initial Solution}}{\text{Signal Final Solution}}$$

Standard addition equation:

$$\frac{[X]_i}{[S]_f + [X]_f} = \frac{I_x}{I_{S+X}} \quad (11)$$

For an initial volume V_o of unknown and added volume V_s , of standard with concentration $[S]_i$, the total volume is $V = V_o + V_s$ and the concentrations in Equation (7) are

$$[X]_f = [X]_i \left(\frac{V_o}{V} \right) \quad [S]_f = [S]_i \left(\frac{V_s}{V} \right) \quad (12)$$

The quotient (initial volume/final volume), which relates final concentration to initial concentration, is called the dilution factor.

By expressing the diluted concentration of analyte, $[X]_f$ in terms of the initial concentration of analyte, $[X]_i$, we can solve for $[X]_i$, because everything else in Equation (7) is known.

For successive standard additions to one solution

$$I_{S+X} \left(\frac{V}{V_o} \right) = I_x + \frac{I_x}{[X]_i} [S]_i \left(\frac{V_s}{V_o} \right) \quad (13)$$

A graph of $I_{S+X} \left(\frac{V}{V_o} \right)$ (the corrected response) on the y-axis versus $[S]_i \left(\frac{V_s}{V_o} \right)$ on the x-axis should be a straight line. The right side of the equation (9) is zero when $[S]_i \left(\frac{V_s}{V_o} \right) = -[X]_i$. The magnitude of the intercept on the x-axis is the original concentration of unknown, $[X]_i$.

Chapter IV: Experimental Procedure

4.1 Preparation of solutions

4.1.1 Preparation of the electrolyte supporting solution

An electrolyte is any substance containing free ions that make it the solution electrically conductive. When electrodes are placed in an electrolyte and a voltage is applied, the electrolyte will conduct electricity. It provides a high ionic strength in such a way that migration of the electroactive species from the bulk solution to the electrode surface is feasible. The most typical electrolyte is an ionic solution, such as Potassium chloride (KCl) or Sodium chloride (NaCl). Electrolyte solutions from 0.1M to 1.0M were prepared by adding the precalculated amount of NaCl (Sigma-Aldrich ACS Reagent 99.9%) and completing with ultrapure deionized water to 1L.

4.1.2 Preparation of the stock solution

An 1mM Cu(II) and 1mM Fe(III) ions stock solutions were prepared by adding the precalculated needed amount of $\text{CuSO}_4 \cdot 5 \text{H}_2\text{O}$ and $\text{FeNH}_4(\text{SO}_4)_2 \cdot 12 \text{H}_2\text{O}$ (Fischer Scientific, ACS Reagent 99.9%, with a FW $249.68 \text{ g}\cdot\text{mol}^{-1}$, and FW $392.14 \text{ g}\cdot\text{mol}^{-1}$, respectively) and completing to 500mL with the electrolyte supporting solution. These stock solutions are used to prepare Cu (II) and Fe (III) ion solutions.

4.2 Sampling and pretreatment of natural seawater

The sample of sea water is collected from the Mayagüez Bay, Road 102 K.m. 4.3, in a clean NAIGENE container at a depth of 6 inches from the surface. The sample is then filtered using a gravity filtration system (Figure 13) to eliminate the solid particulate. A

Whatman N^o.40 commercially paper filter were used. This paper has the following description; 12.5 cm diameters, medium porosity, particle retention 8 μ m, medium flow rate and maximum ash per cycle 0.00011g). After filtering, the samples are store in the refrigerator in order to prevent microorganism proliferation.

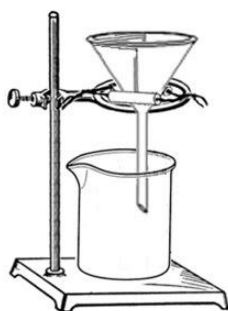


Figure 13. Gravity filtration system

4.3 Measuring chloride concentration of seawater

The concentration of the Chloride ion gives a quick measurement of the salinity of water samples. An ion selective electrode (ISE) was used to determine the concentration of chloride ion (Cl^-), or salinity level in saltwater samples. The electrode used was a Vernier Chloride Ion Selective Electrode (CL-BTA). The ISE was connected to a Vernier Interface Lab Quest. The preparation and calibration method for ISE was followed as described in the “User Manual: Ion Selective Electrode” (e.g. : [35]).



Figure 14. Vernier Chloride Ion Selective Electrode and a Vernier Interface Lab Quest(e.g. : [35]).

4.4 pH determination

A pH meter to determine the pH of the solutions model accumet ® AB 15 plus was used. The electrode is calibrated using commercially available standard buffers.

4.5 Nitrogen gas pretreatment

Dissolved oxygen is an important contaminant in electrochemical experiments. Before recording any cyclic voltammogram, it was necessary to remove any dissolved oxygen in solution by purging with ultra high purity nitrogen gas (99.999% pure, Linde Gas) for five minutes. A 10.0 mL solution was added to the cell via immediately before the CV analysis and purged with nitrogen.

4.6 Pretreatment of the working electrode surface

The condition of the WE surface affects the kinetic of the electron transfer, and its current response. In order to obtain reproducible results, all working electrodes surfaces require a pretreatment before recording a cyclic voltammogram. The most common method for the pretreatment is polishing with 0.05µm alumina powder (BASi) in a Texmet pad. The WE is polished making a continuous number (~20 times) of circular movements over the alumina powder in both direction (clock wise and counter clock wise). Refer to figure 15 for the polishing step. Once polishing has been completed, the electrode surface must be rinsed with ultrapure water (deionized water 18.2 MΩ·cm) to remove all particles of polishing material. It is necessary to rinse with ultrapure water in order to ensure that the trace ion contaminant in tap water will poison the working electrode surface. After the surface electrode has been rinsed, the electrode should

also be sonicated in ultrapure water for a period of 20 seconds to ensure complete removal of any alumina particles.

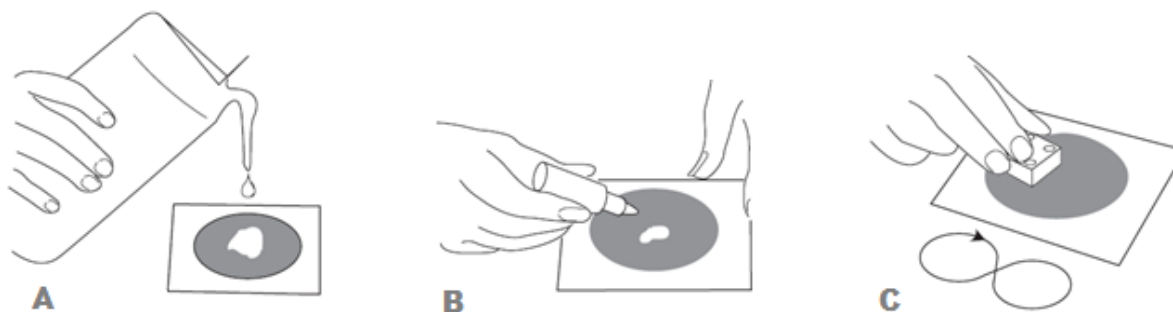


Figure 15. Polishing step for working electrode: **a)** Wet Polishing pad before adding polish powder, **b)** Add a small amount of polish solution (Alumina) to the wet pad, **c)** Use smooth motion and light pressure when polishing.

4.7 Description of the experiments using Cyclic Voltammetry technique

4.7.1 Setting the instrumental parameters

The three electrodes to be use are placed in the electrochemical cell fitted top shown in figure 16. The electrodes are placed so that the working electrode is close to the reference electrode in order to minimize the solution resistant between them, while the auxiliary electrode is placed as far away as possible from the reference electrode. The potential (E) is sweep and measured with the potentiostat vs. the reference electrode, and the generated current (i') do the redox processes occurs in the circuit between the working electrode and the auxiliary electrode as measured with the galvanostat (see fig. 17). The three electrodes were connected to their corresponding instrumental cables. The black, white and red cables correspond to the working, reference, and auxiliary electrodes, respectively, as the design of the BASi C-3 instrument indicates.

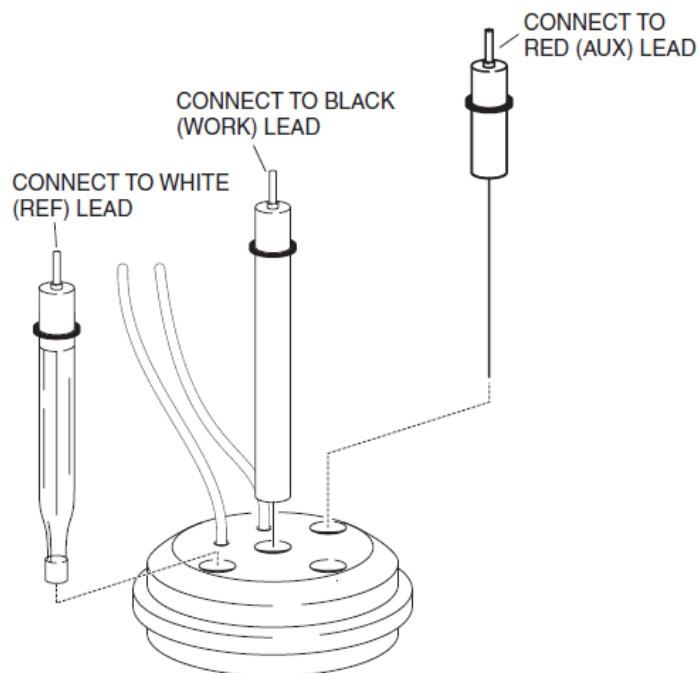


Figure16. Arrangement of three electrode system in a fitted top for a C-3 Cell (e.g. : [2]).

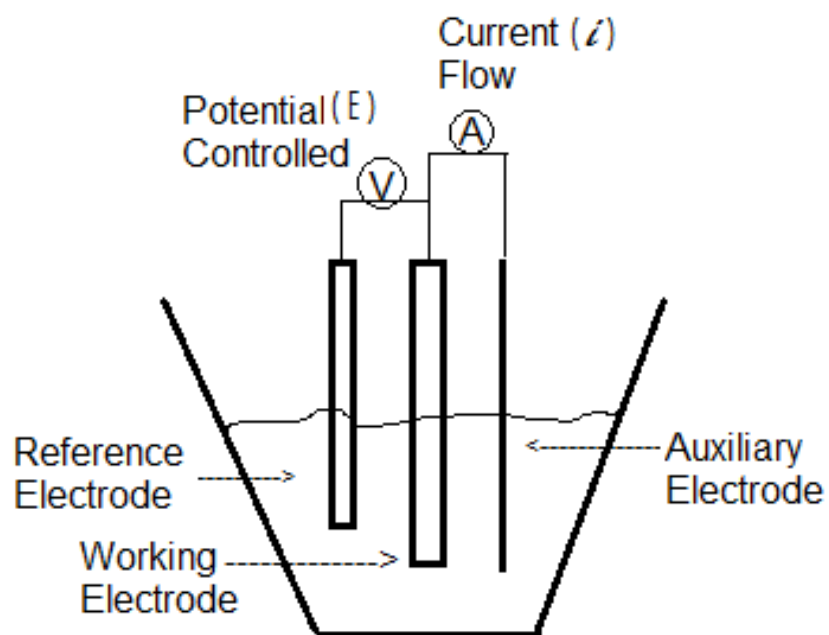


Figure 17. Diagram of the electrical circuitry for potential (E) and current (i).

Before placing the three electrodes in the cell, the potentiostat and the electrochemical cell were turned on. BASi Epsilon-EC Version 2.13.77 software was used. The cyclic voltammetry technique was selected as the operation mode of the BASi Epsilon software. To choose the cyclic voltammetry option it is necessary to choose the “Experiment” icon in the menu bar. Then, make the following selection: Select New Experiment > Cyclic Voltammetry > Select, indicated in the upper bar (fig. 18). Once the cyclic voltammetry is technique is selected, the CV Parameters window appears and the desired parameters are specified. An alternative form to open the CV parameters windows can be done by selecting the Experiment icon in the menu bar and then, Change Parameters is selects.

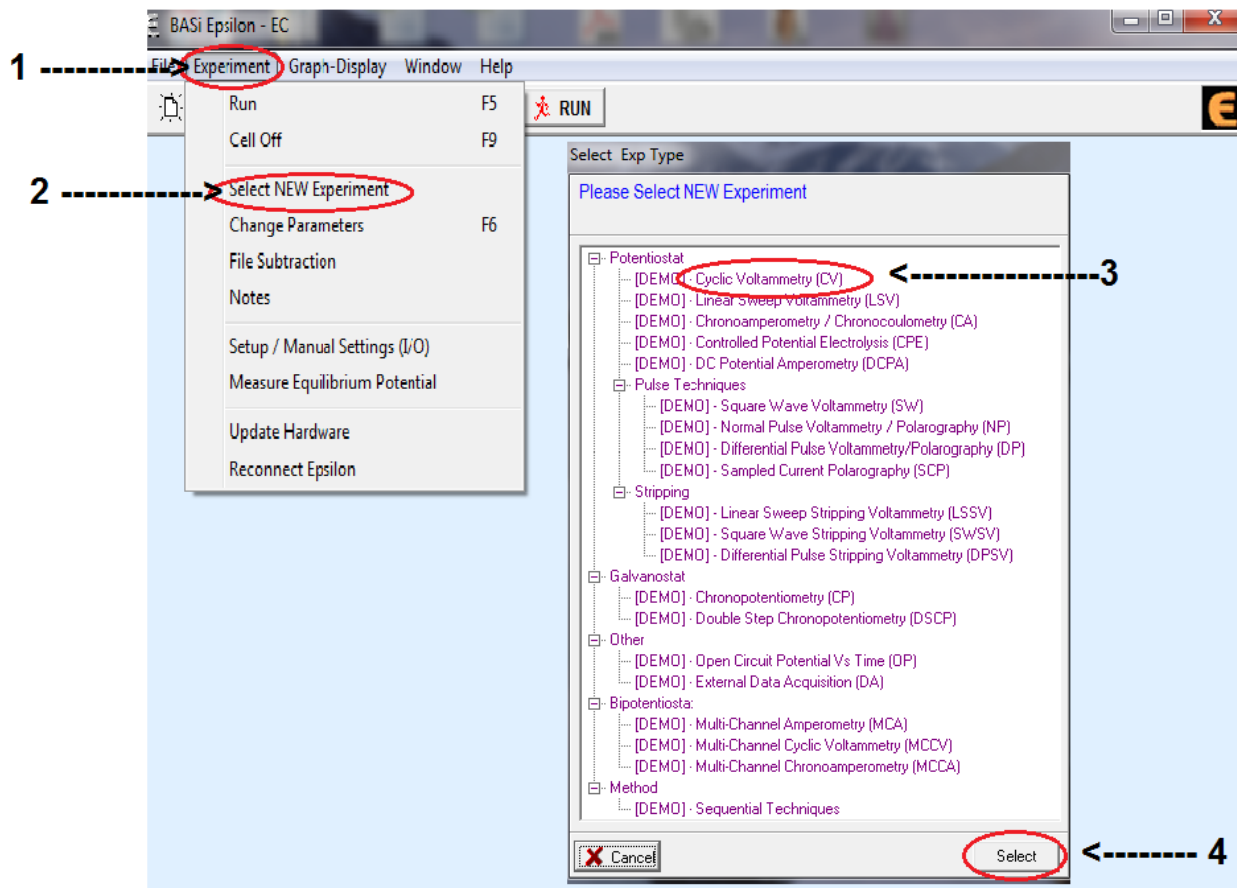


Figure 18. Sequence of steps for the initiation of the CV programs.

General parameters need to be specified in order to run desired CV experiments. These parameters are:

- the limit of the potential window which is the range of voltage used in millivolts, (mV). Example from -1000mV (Initial Potential) to +1000mV (switching potential).
- scan rate which is the velocity of sweep in millivolts per second (mVs^{-1})
- number of segments (2 segments are equal to one complete cycle),
- sensitivity in a range of 100 microAmpere per Volts (μAV^{-1}) to 1 nanoAmpere per Volts (nAV^{-1}). The sensitivity is a parameter that is determined experimentally.

The most frequently sensitivity used is 10 micro Ampere per Volts (μAV^{-1}).

Figure 19 illustrates a typical CV parameter window. The limits of the potential windows describe the initial potential, the switching potential (voltage value at which the sweeping direction is reversed) and the final potential. The direction of the initial scan may be either toward negative or positive voltage, depending on the composition of the sample and/or the desired redox reaction. The potential at which reversal takes place is called switching potential. These parameters are choosing according to the experimental design needed.

Initial Potential (mV)	-1000	# of Segments	4
Switching Potential 1 (mV)	1000	Scan Rate (mV/s)	100
Switching Potential 2 (mV)	-1000	Quiet Time (Sec)	2
Final Potential (mV)	-1000	Full Scale (+/-)	1 uA

☐ Apply Open Circuit Potential for Initial E
☐ Run - External Trigger

Filter / F.S. MR Cell

RUN IR-COMP Apply Exit

Figure 19. General CV Parameters box corresponding to the BASi Epsilon EC software version 2.13.77, 2009, Bionalytical System, Inc. showing a typical set of parameters.

Chapter V: Results and Discussion

5.1 Natural water parameters

Salinity is the total salts dissolved in water, expressed, either as mg/L (equal to parts per million, ppm) or in ng/L (parts per thousand, ppt). Using a Cl^- ion selective electrode the Salinity can be calculated using the following formula:

$$\text{Salinity} \left(\frac{\text{mg}}{\text{L}} \right) = 1.8066 \left([\text{Cl}^-], \frac{\text{mg}}{\text{L}} \right) \quad (14)$$

The level of salinity in parts per thousand would be:

$$\text{Salinity} (\text{ppt}) = 1.8066 \left([\text{Cl}^-], \frac{\text{mg}}{\text{L}} \right) \left(\frac{1}{1000} \right) \quad (15)$$

Using the Cl^- ion selective electrode, the chloride ion measured was 14,625 mg/L. Using the salinity equation 14, the seawater salinity used in our experiment was 26,421 mgL^{-1} (or 26 ppt), as determine using the Cl^- ion selective electrode. On the other hand, pH (power of Hydrogen) is simply a measurement of the acidity or alkalinity of a solution. The seawater pH at 25°C (room temperature) was measured to be 8.07. The generally accepted pH level in a basic saltwater system is between 7.6 and 8.4 and our value lies within this range.

Table 4. Mayaguez coast seawater parameters.

Parameters	Seawater
pH	8.07
Salinity	26 ppt

5.2 Selecting the working electrode

The first stage of our research was to determine the appropriate working electrode for the determination of $\text{Cu}^{+2}/\text{Cu}^{+1}$ ions and $\text{Fe}^{+3}/\text{Fe}^{+2}$ ions system in order to be able to analyze their content in natural waters.

5.2.1 Platinum Electrode (PtE)

Choosing an appropriate working electrode is vital for Cyclic Voltammetry experiments. Platinum (Pt) electrode is recommended for organic or inorganic substances measurement because they have high overpotential for oxygen evolution and low overpotential for hydrogen evolution. Figure 20 shows a typical voltammogram of a clean Pt electrode in a 0.5M H_2SO_4 solution with an initial scan direction toward the positive direction and a potential window from +1300mV to -300mV.

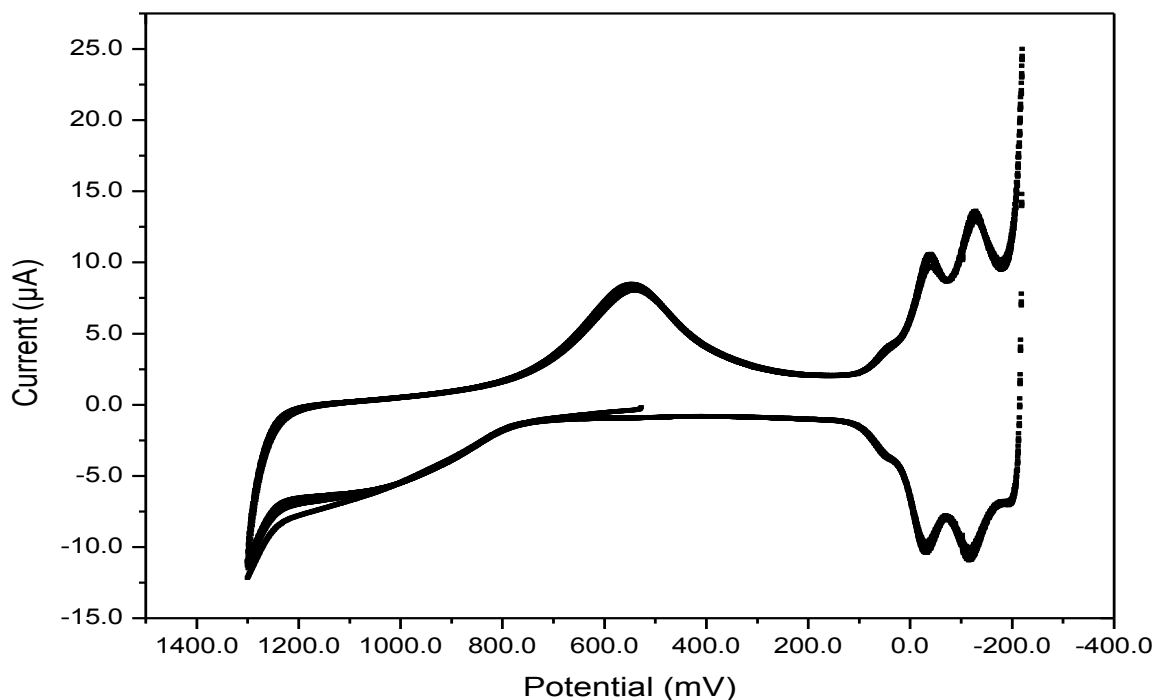


Figure 20. Cyclic voltammogram using a BASi Platinum electrode in a 0.5M H_2SO_4 solution at a scan rate of 100mVs^{-1} and sensitivity $100\mu\text{A}$.

The shape, number and size of the Pt peaks depend on the pretreatment of the electrode, solution impurities and supporting electrode. A smooth Pt electrode in 0.5M H₂SO₄ solution has various regions (refer to figure 21). As the potential region become more positive, the current is attributed to the formation of adsorbed oxygen or platinum oxide. The peak marked with the number “2” in figure 21 represents the oxygen evolution. While the peak marked with the number “1” corresponds to the hydrogen evolution.

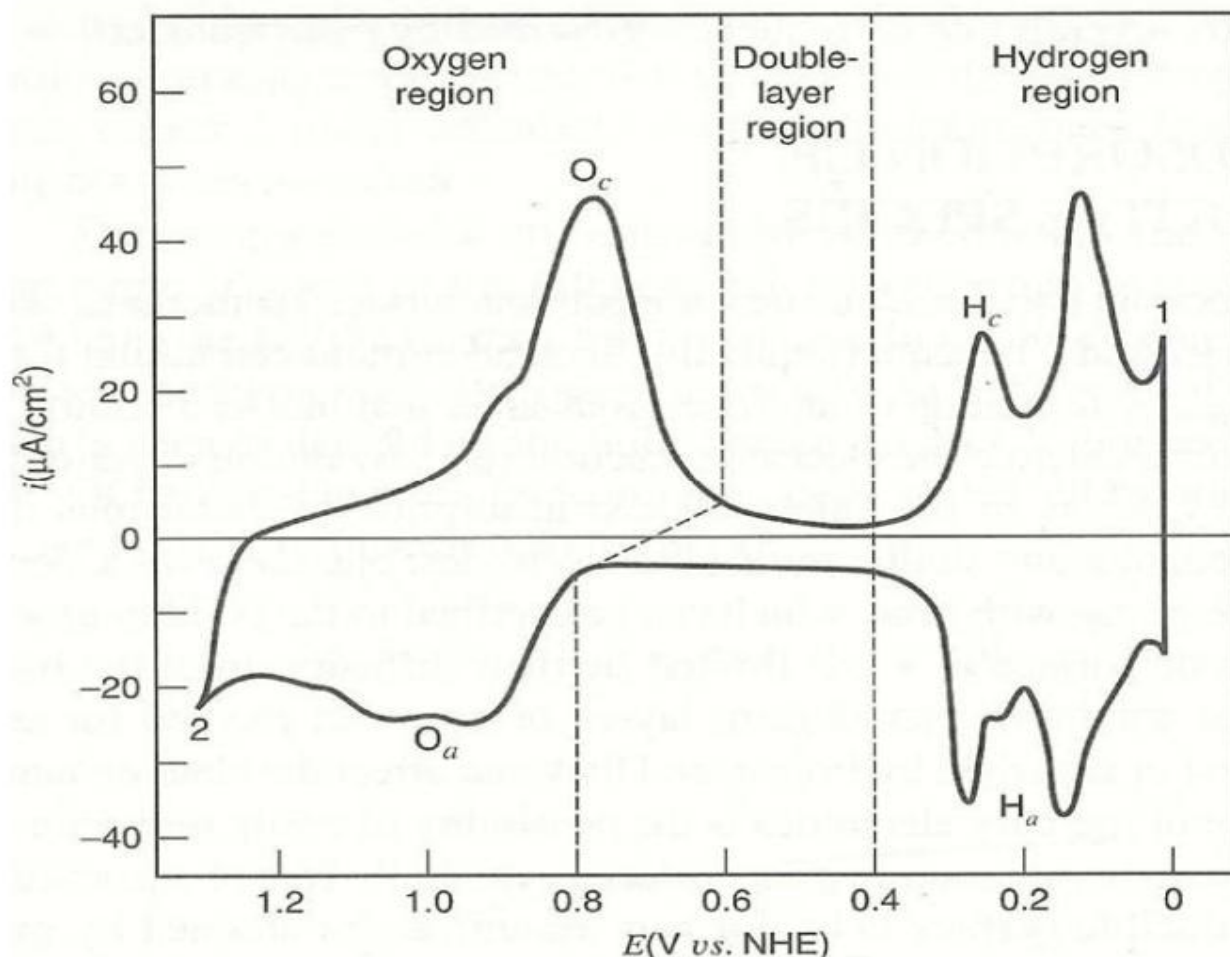


Figure 21. Cyclic voltammogram for a smooth Pt electrode in 0.5M H₂SO₄ solution. (e.g: [34])

Once with an established behavior of our clean Pt electrode surface (see fig. 20), we were ready to study the possibility of using this electrode for the analysis of our Cu^{+2} and Fe^{+3} ions solution. Figure 22 shows the cyclic voltammogram of 1mM Cu^{+2} in 0.1M NaCl electrolyte supporting solution with a potential window from +650mV to +0mV at a scan rate of 100mV/s and a sensitivity of $10\mu\text{AV}^{-1}$ with Ag/AgCl as the reference electrode in a negative initial scan direction (isd). In this figure we can observed the reduction of Cu^{+2} to Cu^{+1} and Cu^{+1} to Cu metal, and in the reverse direction we can observe a reversible process for both reductions, when the two peak of oxidation of Cu metal to Cu^{+1} and Cu^{+1} to Cu^{+2} .

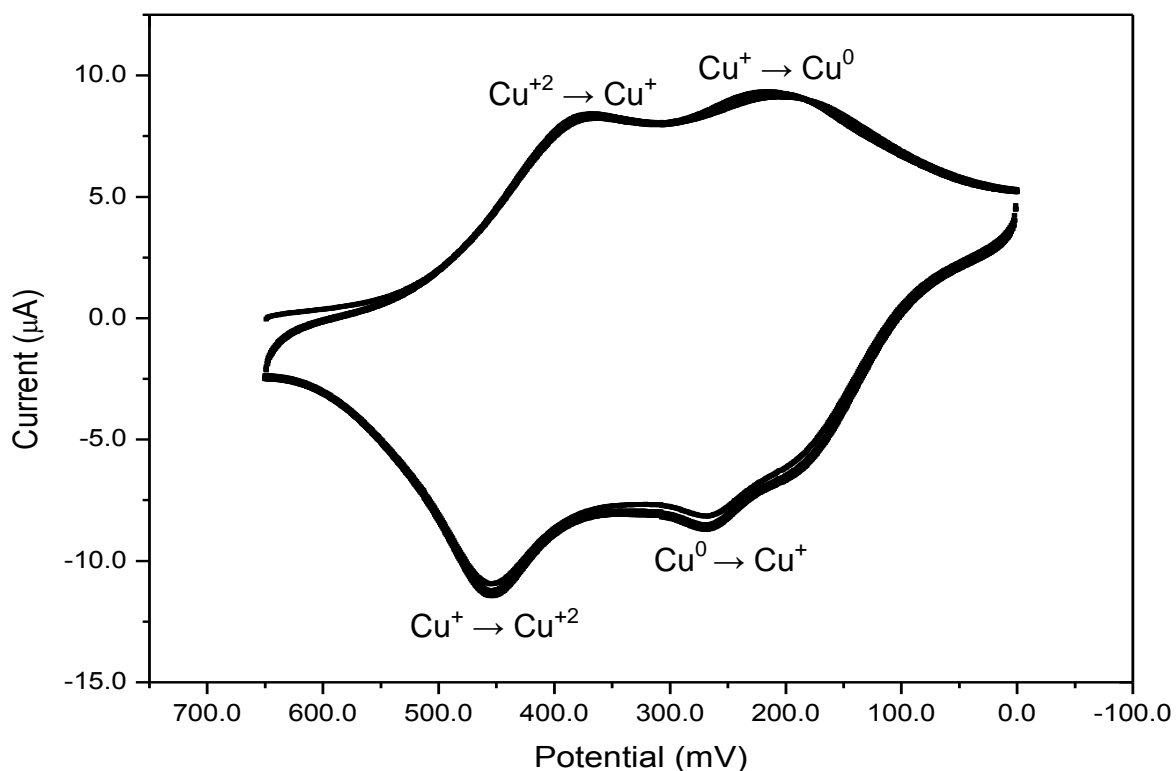


Figure 22. Voltammogram of 1mM Cu^{+2} in 0.1M NaCl electrolyte supporting solution with a potential window from +650mV to +0mV at a scan rate of 100mV/s and a sensitivity of $10\mu\text{AV}^{-1}$ with Ag/AgCl as the reference electrode and Pt as the working electrode.

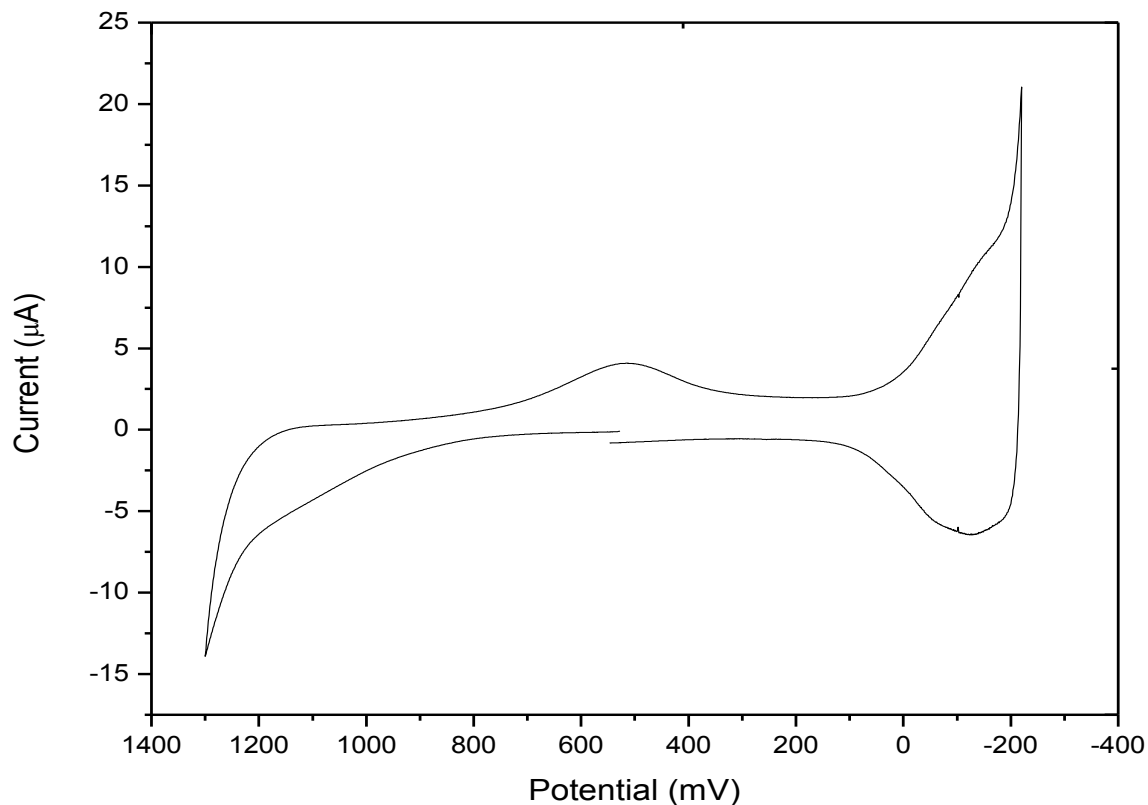


Figure23. Voltammogram of Pt electrode in 0.5M H₂SO₄ solution. Scan rate 100mVs⁻¹ and sensitivity 100μAV⁻¹. This electrode was previously used for the analysis of Cu⁺² in 0.1M NaCl electrolyte supporting solution.

The Pt surface once we have run the voltammogram for Cu⁺² ion in 0.1M NaCl electrolyte supporting solution, the electrode suffer a surface modification as it can be seen in figure 23, when the details of the hydrogen evolution peak almost disappear indicating Cu metal deposition over the Pt electrode surface. This situation was considered in order to change the electrode of our experiment to GC electrode.

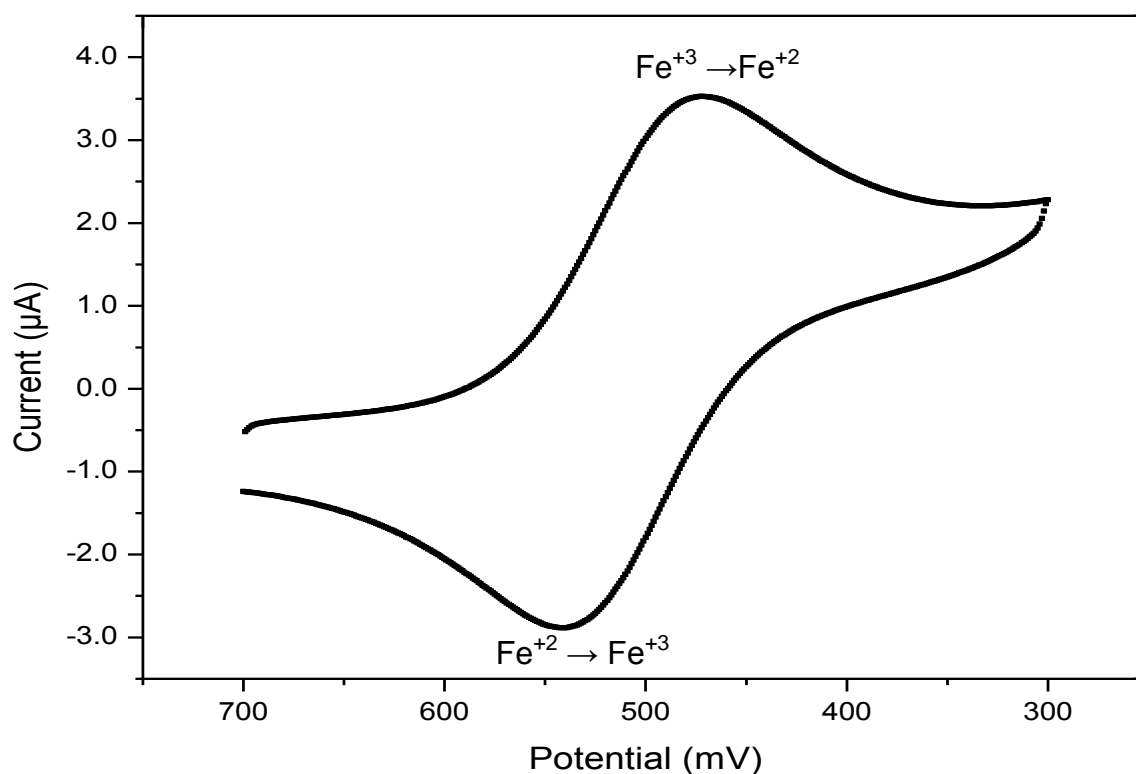


Figure 24. Voltammogram of 1mM Fe^{+3} with a potential window from +750mV to +250mV at a scan rate of 100mV/s and a sensitivity of $10\mu\text{AV}^{-1}$ with Ag/AgCl as the reference electrode.

However, Pt electrode is adequate for $\text{Fe}^{+3}/\text{Fe}^{+2}$ ions analysis because the redox process can be analyzed in the potential window from 700 to 300mV using a sensitivity of $10\mu\text{AV}^{-1}$, refer to figure 24.

5.2.2 Glassy Carbon Electrode (GCE)

The GC working electrode is widely used, and it's considered to be an inert electrode for Hydronium ion reduction in aqueous solution. The GC working electrode is appropriate for the analysis of Cu ions because it allows the study of the redox processes of Cu ions. A full voltammogram of 1mM Cu (II) in 0.1M NaCl electrolyte supporting solution will be discussed in section 5.3.

The use of GC working electrode is not appropriate for the analysis of $\text{Fe}^{+3}/\text{Fe}^{+2}$ ions solutions. As figure 25 shows, only the reduction peak of Fe^{+3} to Fe^{+2} was observed, while the redox peaks are better defined when using the Pt working electrode, refer to figure 24.

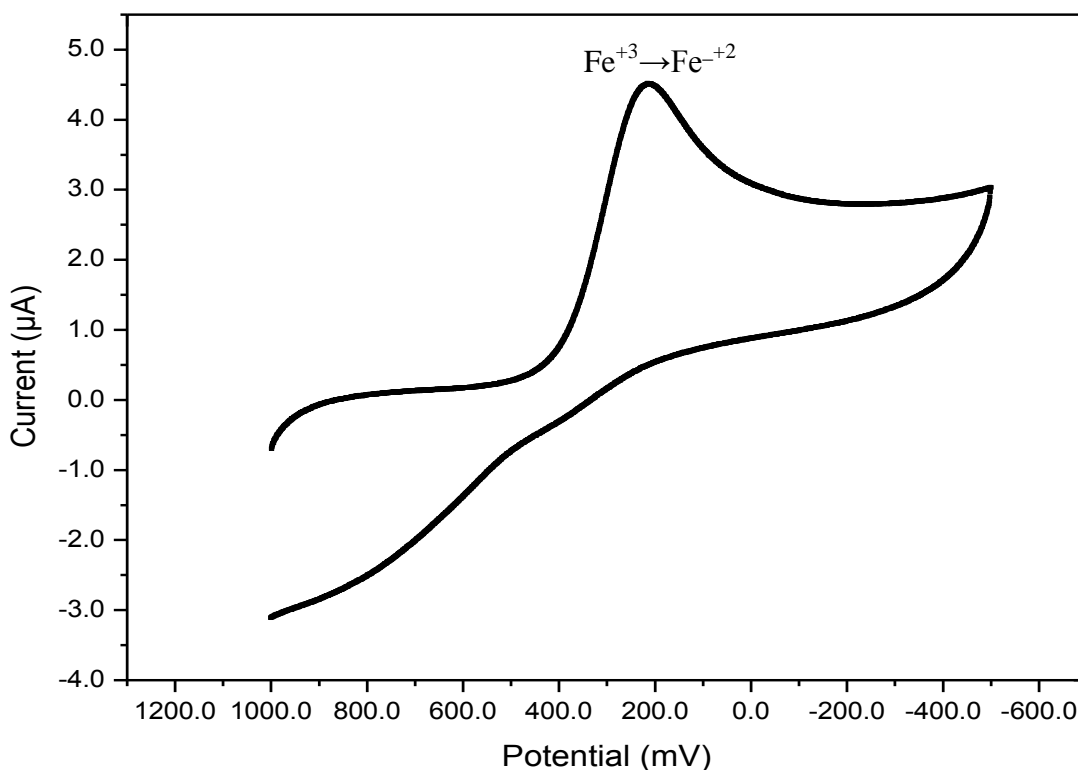


Figure 25. Voltammogram of 1mM Fe^{+3} in 0.1M NaCl electrolyte supporting solution with a potential window from +1000mV to -600mV at a scan rate of 100mVs^{-1} and a sensitivity of $10\mu\text{AV}^{-1}$ with Ag/AgCl as the reference electrode and GC as working electrode.

After these preliminary experiments it was desired to use the GC working electrode for the analysis of Cu^{+2} ion and Pt working electrode for the analysis of Fe^{+3} ion in natural waters.

5.3. Selecting a working voltage window and peak location for the analysis of Cu^{+2} and Fe^{+3} ions

A working voltage window is a region in the voltammogram where the reduction and oxidation peaks of our interest does not overlap with any other reduction or oxidation peaks of any other electrolyte in our solution of interest.

5.3.1 Copper (II) ion analysis

A full voltammogram of 1mM Cu (II) stock solution in 0.1M NaCl electrolyte supporting solution using GC electrode allows to study the voltage at which the redox peaks appears in the cyclic voltammogram. Using a potential window from +400 mV to -700 mV scanning toward the negative direction, two distinctive electrochemical redox peaks appears (fig. 26), one at approximately +87 mV and another one at -445 mV vs. Ag/AgCl reference electrodes. These two peaks were ascribed to the reduction peak of Cu^{+2} to Cu^{+} and Cu^{+} to Cu^0 (copper metal), respectively. While, in the reverse scan direction toward a more positive voltage, two signals appears approximately at -25 mV and +151 mV, assigned as the oxidation peak of Cu^0 to Cu^{+} and Cu^{+} to Cu^{+2} , respectively. The sharp peak of Cu^0 to Cu^{+1} at 25mV is a typical peak of an adsorbed metal on the GC electrode surface. In figure 26, the sharp peak represents the electrodeposition of a thin layer of copper metal in the electrode surface. This potential window, +400mV to -700mV, allow us to study the complete redox process of the Cu ions. A narrow potential window was selected to carry out our further experiments in order to avoid the modification of the electrode surface with a thin layer of Cu^0 in its surface electrode.

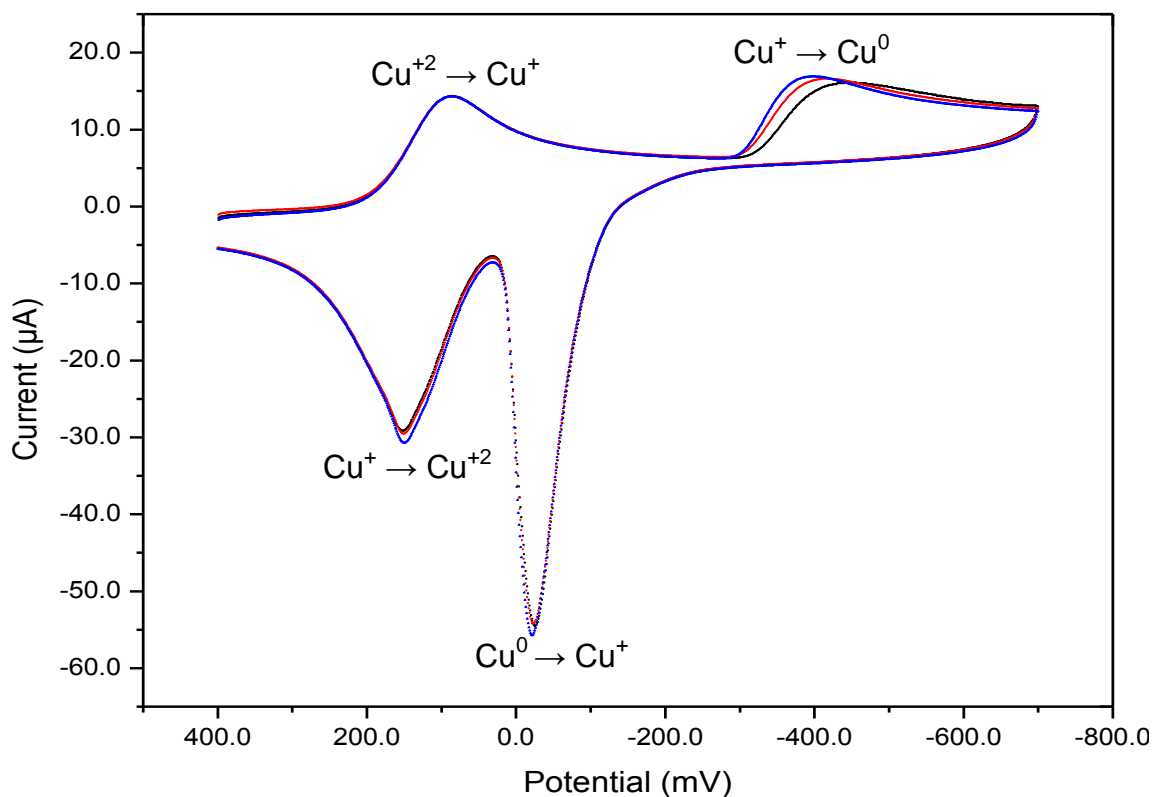


Figure 26. Voltammogram of 1mM Cu^{+2} in 0.1M NaCl solution with a potential window from +400mV to -700mV at $100\text{mV}\cdot\text{s}^{-1}$ at a sensitivity of $100\mu\text{AV}^{-1}$ with Ag/AgCl reference electrode and using GC electrode.

The potential window selected for this work was from +300 mV to -100 mV with a negative initial scan direction. Using this potential window, only the reduction of Cu^{+2} to Cu^{+} is allowed between this limit (see fig. 27).

Figure 27 shows ten independent voltammograms of Cu^{+2} ion in 0.1 NaCl electrolyte supporting solution, these ten independent voltammograms were used to determine the location of our peak of interest as an average of ten experiments using GC working electrode, Ag/AgCl as the reference electrode, at a scan rate of $100\text{mV}\cdot\text{s}^{-1}$ and with a

sensitivity of $100\mu\text{A}\text{V}^{-1}$ toward a more negative direction. Table 5 Summarize the Cu^{+2} to Cu^{+} redox parameters of the ten samples studied.

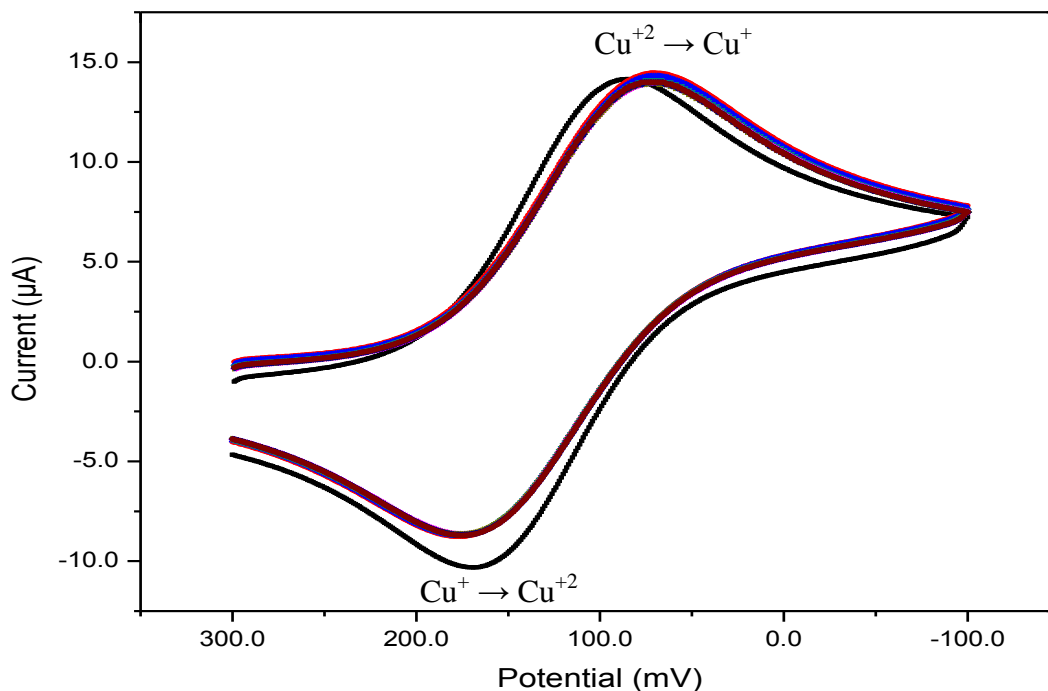


Figure 27. Voltammogram of 1mM Cu^{+2} with a potential window from +300mV to -100mV at 100mV/s and a sensitivity of $100\mu\text{A}$ with Ag/AgCl as the reference electrode.

Table 5. Potential and Current of the Cu^{+2} to Cu^{+1} redox process of the ten samples studied.

Sample	E_{pc} (mV)	i_{pc} (μA)	E_{pa} (mV)	i_{pa} (μA)
1	85	13.4	169	-11.9
2	86	14.8	169	-10.0
3	85	14.1	169	-10.3
4	71	14.5	177	-8.8
5	71	14.3	175	-8.7
6	71	14.1	176	-8.7
7	71	14.0	176	-8.6
8	73	13.9	174	-8.6
9	71	14.0	175	-8.6
10	72	14.1	175	-8.7
Average	75 (± 7)		174 (± 3)	
SD	6.6		3.2	
RSD (%)	8.9		1.8	

Using this potential window, +300 mV to -100 mV, toward a more negative direction only one peak, Cu^{+2} to Cu^{+1} , at approximately +75(\pm 7) mV is obtained. While in the reverse scan, toward a more positive direction, one oxidation peak, Cu^{+} to Cu^{+2} , at approximately 174 (\pm 3) mV is observed.

5.3.2 Iron (III) ion analysis

A full voltammogram of 1mM Fe (III) stock solution in 0.1NaCl electrolyte supporting solution using Pt working electrode allows to study the voltage at which the redox peaks appears in the cyclic voltammogram. Using a potential window from +750mV to +250mV scanning toward the negative direction, one distinctive electrochemical redox peaks appears at approximately +479 (\pm 14) mV vs. Ag/AgCl reference electrodes which were ascribed to the reduction peak of Fe^{+3} to Fe^{+2} (fig. 28). While, in the reverse scan direction toward a more positive voltage, one peak appears approximately at +553 (\pm 11) mV, attributed to the oxidation of Fe^{+2} to Fe^{+3} . This potential window allows us to study the redox process of the Fe^{+3} / Fe^{+2} ions.

Figure 28 shows ten independent voltammograms of Fe^{+3} ion solution, these ten independent voltammogram was used to determine the location of our peak of interest as an average of ten experiments using Pt as the working electrode, Ag/AgCl as the reference electrode, at a scan rate of $100\text{mV}\cdot\text{s}^{-1}$ and with a sensitivity of 10uAV^{-1} . Table 6 summarize the Fe^{+3} to Fe^{+2} redox parameters of the ten individual samples analyzed.

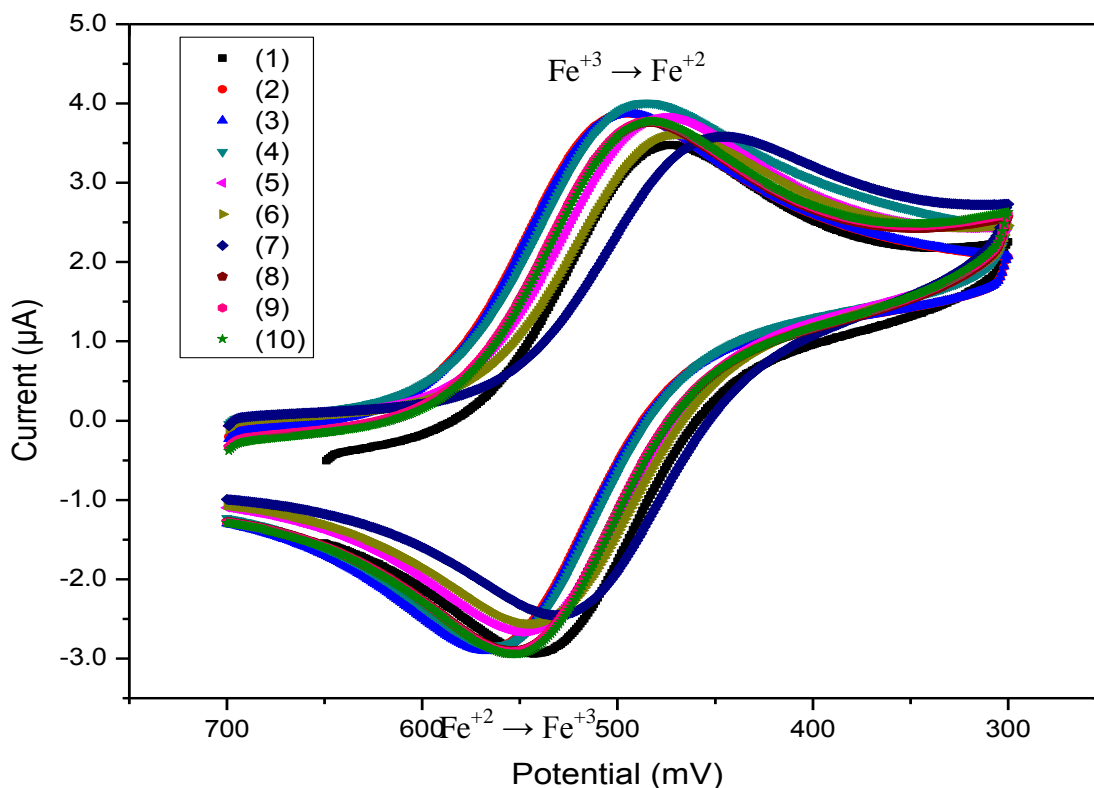


Figure 28. Voltammogram of 1mM Fe^{+3} with a potential window from +700mV to +250mV at 100mV/s and a sensitivity of $10\mu\text{AV}^{-1}$ with Ag/AgCl reference electrode and using PT working electrode.

Table 6. Potential and Current of the Fe^{+3} to Fe^{+2} redox processes of the ten samples studied.

Sample	E_{pc} (mV)	i_{pc} (μA)	E_{pa} (mV)	i_{pa} (μA)
1	473	1.6907	543	2.4842
2	495	2.8629	567	3.4501
3	495	3.0573	567	3.4592
4	485	3.5679	562	3.2886
5	475	3.4672	549	2.7259
6	468	3.2914	544	2.4775
7	447	3.2068	532	1.5549
8	484	3.4119	554	2.7192
9	484	3.4513	554	3.4513
10	482	3.4748	554	2.3070
Average	479 (± 14)		553 (± 11)	
SD	14.2		11.1	
RSD (%)	3.0		2.0	

5.4 Selecting the sensitivity for the analysis of Cu^{+2} and Fe^{+3} ions.

The sensitivity is the scale in the voltammogram to magnify the measured signal (Amperometric current) versus the applied potential. The CV instruments have a scale values in decades from 100 mA to 1nA per volts. The sensitivity is adjusted in order to analyze the peaks of interest. For the analysis of 1mM Cu (II) stock solution a sensitivity of $100\mu\text{AV}^{-1}$ was used, while for 1mM Fe (III) stock solution a sensitivity of $10\mu\text{AV}^{-1}$ was used. A sensitivity of $100\mu\text{AV}^{-1}$ means that the current scale is up to a maximum of 100 μA , while a sensitivity of $10\mu\text{AV}^{-1}$ is reduce up to a current scale maximum of 10 μA . When the solutions to be analyzed are of concentration lowers than 0.1mM a more sensitive scale is required. For the analysis of the seawater a sensitivity of a $1\mu\text{AV}^{-1}$ was used. This sensitivity allows to obtain a higher magnification of the signal scale.

5.5 Effect of the scan rate on the Cu^{+2} and Fe^{+3} ion redox waves.

The scan rate is the rate in which the ions diffuse into the surface electrode. It's the time taken to sweep the potential window per second. Depending of the rate of the redox process, the scan rate can be selected from 10mVs^{-1} up to $25,000\text{mV}^{-1}$. Figure 29 shows the behavior of the Cu (II) and Fe (III) ions redox peaks studied at seven different scan rates: $10\text{ mV}\cdot\text{s}^{-1}$, $50\text{ mV}\cdot\text{s}^{-1}$, $100\text{ mV}\cdot\text{s}^{-1}$, $300\text{ mV}\cdot\text{s}^{-1}$, $500\text{ mV}\cdot\text{s}^{-1}$, $700\text{ mV}\cdot\text{s}^{-1}$ and $1000\text{ mV}\cdot\text{s}^{-1}$. For each individual scan rate the electrode surface was removed and cleaned but used in the same solution. As it was expected, the peak maximum current increases with an increase in the scan rate.

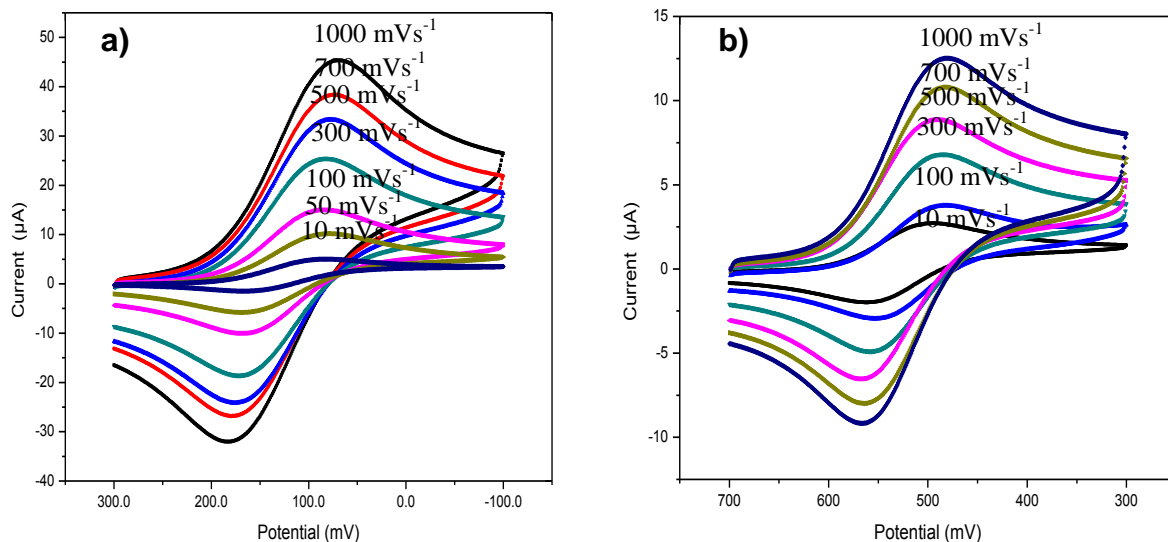


Figure 29. Cyclic voltammograms of **a)** 1 mM Cu⁺² in 0.1M NaCl electrolyte supporting solution and **b)** 1mM Fe⁺³ electrolyte supporting solution at different scan rate from 10 mV·s⁻¹ up to 1000 mV·s⁻¹ and at sensitivity of 100μAV⁻¹.

Figures 30 show a linear behavior for Cu (II) and Fe (III) ions, respectively. The theoretical Randles-Sevcik treatment postulate that when plotting the peak current obtained as a function of the square root of the scan rate ($v^{1/2}$), a linear behavior should be obtained. The Randles-Sevcik equation at room temperature is:

$$i = 2.69 \times 10^{-8} n^{3/2} A D^{1/2} C^* v^{1/2} \quad (16)$$

where A is the cross section area of the electrode (cm²),

C^* is the bulk concentration of the reduced or oxidize species,

D is the diffusion coefficient of the reduced or oxidize species,

v is the scan rate,

n is the number of electrons transferred

The theoretical treatment data for the Cu (II) and Fe (III) ions are summarized in table 7.

Table 7. Potential and current at seven different scan rate for Cu^{+2} and Fe^{+3} ions in 0.1M NaCl electrolyte supporting solution using Cyclic Voltammetry Technique.

Ion	Scan Rate ($\text{mV}\cdot\text{s}^{-1}$)	Root Square Scan Rate	Cathodic Potential E_{pc} (mV)	Cathodic Current i_{pc} (A)	Anodic Potential E_{pa} (mV)	Anodic Current i_{pa} (A)
Cu (II)	1000	32	69	45	183	-32
	700	27	74	38	179	-27
	500	22	78	33	176	-24
	300	17	83	25	171	-19
	100	10	85	15	169	-10
	50	7	82	11	146	-15
	10	3	98	4	171	-4
Fe (III)	1000	32	388	3.3	554	5.3
	700	27	402	4.4	544	5.0
	500	22	414	3.5	542	4.4
	300	17	420	3.4	535	4.0
	100	10	429	2.1	529	2.1
	50	7	440	1.2	524	1.4
	10	3	448	1.1	518	0.6

Figure 30.a and 30.b show the effect of the scan rate on the peak height of Cu (II) reduction to Copper (I) and Fe (III) reduction to Fe (II), respectively. A linear increment is observed for the reduction current peak due to the increment in the square root of the scan rate both for Cu (II) and Fe (III), respectively. Also, a small displacement in the potential peak is observed due to the variation in the electrode surface as the sequences of the experiment are performance.

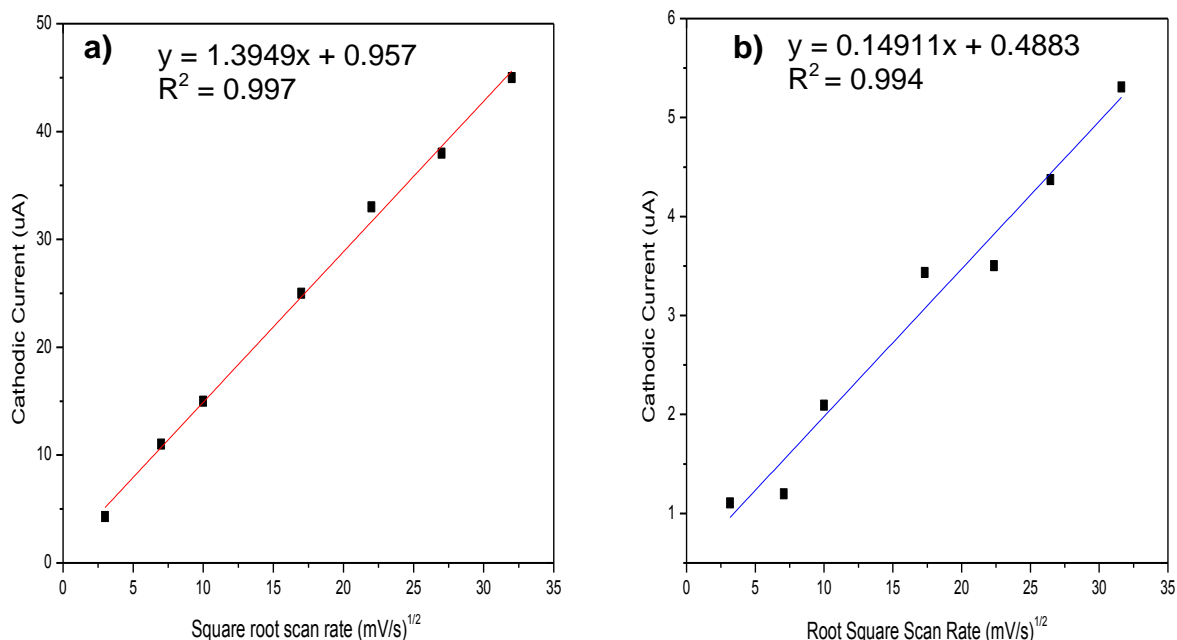


Figure 30. Effect of the scan rate on the peak height of the **a)** Cu^{+2} stock solution and, **b)** Fe^{+3} stock solution.

The linear regressions for these data allow the determination of the representing equation for these experiments. For Cu (II) the straight line $y = 1.3949x + 0.957$ with slope $m = 1.3949$ and for Fe (III) the straight line is $y = 0.1491x + 0.4883$ with slope $m = 0.1491$.

5.6 Reversibility determination in the redox processes

If a redox system remains in equilibrium throughout the potential scan, the redox process is said to be *reversible*. A system at equilibrium requires that the surface concentrations of oxide specie (O) and reduced species (R) are maintained at the values required by the Nernst Equation. The parameter used to determine the reversibility of a reversible process are the peak potential separation ($\Delta E_p = |E_{cathodic} - E_{anodic}|$) at 25°C , lies within the range of 60 to 90mV and the peak current ratio is the unity ($i_{pa}/i_{pc} = 1$).

The peak potential separation for 1mM Cu (II) solution, in a potential window from +0.60V to -0.10V at 500mV/s and a sensitivity of $100\mu\text{AV}^{-1}$ with Ag/AgCl as the reference electrode, is 84mV which lies within the range of reversibility (60 to 90mV) indicating that the Cu (II) redox process is reversible. The peak current ratio determined in our experiment was 0.96 which approximates 1.0, confirming reversibility, once again.

The peak potential separation for 1mM Fe(III) solution, in a potential window from +700mV to +300mV at a scan rate of 100mVs^{-1} and a sensitivity of $10\mu\text{AV}^{-1}$ with Ag/AgCl as the reference electrode, was 70mV, which also lies within the range of reversibility (60 to 90mV). This mean that the Fe(III) redox process is reversible. Also, the peak current ratio measured for Fe (III) was 0.82, which approximates 1.0, confirming reversibility. Reversibility data for both ions is summarizing in table 8.

Table 8. Peak separation ΔE_p and peak current ratio 1mM Cu^{+2} and 1mM Fe (III) in 0.1M NaCl supporting electrolytsolution.

Metal	Peak	Potential (mV)	Current , i (μA)	ΔE_p (mV)	Peak current ratio
Cu (II)	Reduction	85	13.4	84	0.96
	Oxidation	169	-13.0		
Fe (III)	Reduction	479	3.5	70	0.87
	Oxidation	553	-2.9		

5.7 Calculating the number of electrons transferred in the redox process.

The number of electrons transferred in a reversible reduction process of 1mM Cu⁺² in 0.1M NaCl supporting electrolyte solution can be obtained with the application of the following equation:

$$E_{pa} = E_{1/2} + \frac{RT}{nF} \log \left(\frac{i_l - i}{i} \right) \quad (17)$$

where E_{pa} refers to the applied potential with corresponding measured current(*i*) in the negative direction (toward more negative or reduction potential) until limiting reduction current is obtained.

Plotting E_{pa} vs. Log((*i*_l - *i*) / *i*), we can determine the number of electrons transferred.

Figure 31. shows the obtained data region that it's presented e in table 9 and 10.

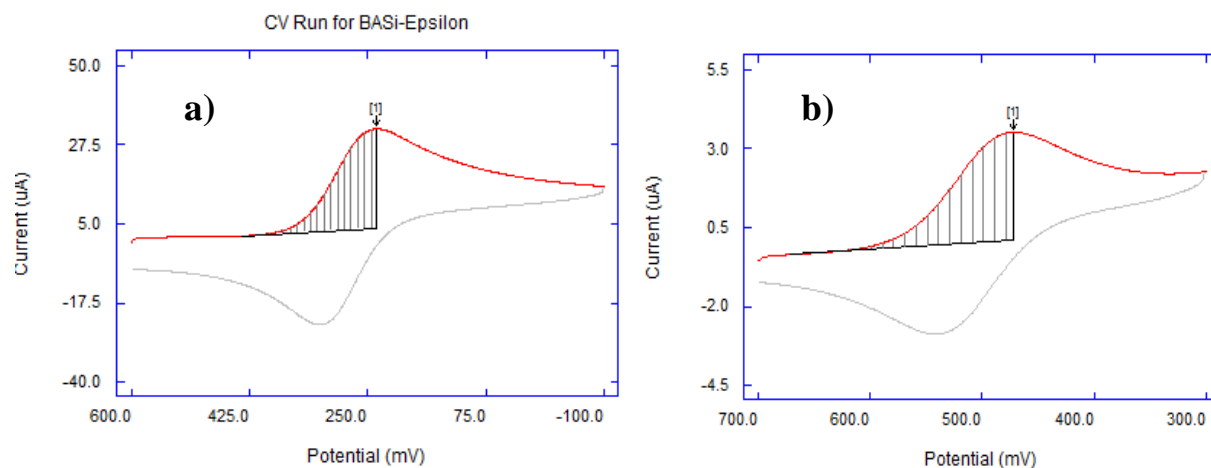


Figure 31. Cyclic voltammogram of **a)** 1mM Cu⁺² in 0.1M NaCl electrolyte supporting solution at a sensitivity of 100μAV⁻¹ and **b)** 1mM Fe⁺³ in 0.1M NaCl electrolyte supporting solution at a sensitivity of 10μAV⁻¹, representing the area selected to determine the number of electrons transferred.

Table 9. Potential (E_{pc}), limiting current (i_l), current (i) and required calculations to obtain $\log(\text{abs}(i_l - i)/i)$ for the reduction process of 1mM Cu^{+2} in 0.1M NaCl electrolyte supporting solution using +300mV to -100mV, Ag/AgCl reference electrode a $100\text{mV}\cdot\text{s}^{-1}$ and $100\mu\text{AV}^{-1}$.

E_{pc}, V	i_l, A	i, A	$(i_l - i)/i$	$\log(\text{abs}(i_l - i)/i)$
8.50E-02	1.50E-05	1.50E-05	0.00E+00	undefined
9.00E-02	1.50E-05	1.50E-05	0.00E+00	undefined
9.50E-02	1.50E-05	1.48E-05	1.35E-02	-1.87
1.00E-01	1.50E-05	1.45E-05	3.45E-02	-1.46
1.05E-01	1.50E-05	1.42E-05	5.63E-02	-1.25
1.10E-01	1.50E-05	1.37E-05	9.49E-02	-1.02
1.15E-01	1.50E-05	1.31E-05	1.45E-01	-0.84
1.20E-01	1.50E-05	1.24E-05	2.10E-01	-0.68
1.25E-01	1.50E-05	1.16E-05	2.93E-01	-0.53
1.30E-01	1.50E-05	1.08E-05	3.89E-01	-0.41
1.35E-01	1.50E-05	9.93E-06	5.11E-01	-0.29
1.40E-01	1.50E-05	9.07E-06	6.54E-01	-0.18
1.45E-01	1.50E-05	8.22E-06	8.25E-01	-0.08
1.50E-01	1.50E-05	7.39E-06	1.03E+00	0.01
1.55E-01	1.50E-05	6.60E-06	1.27E+00	0.10
1.60E-01	1.50E-05	5.87E-06	1.56E+00	0.19
1.65E-01	1.50E-05	5.18E-06	1.90E+00	0.28
1.70E-01	1.50E-05	4.56E-06	2.29E+00	0.36
1.75E-01	1.50E-05	3.99E-06	2.76E+00	0.44
1.80E-01	1.50E-05	3.48E-06	3.31E+00	0.52
1.85E-01	1.50E-05	3.03E-06	3.95E+00	0.60
1.90E-01	1.50E-05	2.63E-06	4.70E+00	0.67
1.95E-01	1.50E-05	2.29E-06	5.55E+00	0.74
2.00E-01	1.50E-05	1.99E-06	6.54E+00	0.82
2.05E-01	1.50E-05	1.73E-06	7.67E+00	0.88
2.10E-01	1.50E-05	1.50E-06	9.00E+00	0.95
2.15E-01	1.50E-05	1.32E-06	1.04E+01	1.02
2.20E-01	1.50E-05	1.15E-06	1.20E+01	1.08
2.25E-01	1.50E-05	1.01E-06	1.39E+01	1.14
2.30E-01	1.50E-05	8.85E-07	1.59E+01	1.20
2.35E-01	1.50E-05	7.84E-07	1.81E+01	1.26
2.40E-01	1.50E-05	7.11E-07	2.01E+01	1.30
2.45E-01	1.50E-05	6.20E-07	2.32E+01	1.37

Table 10. Potential (E_{pc}), limiting current (i_l), current (i) and required calculations to obtain $\log(\text{abs}(i_l - i)/i)$ for the reduction process of 1mM Fe^{+3} in 0.1M NaCl electrolyte supporting solution using +700mV to +300mV, Ag/AgCl reference electrode a $100\text{mV}\cdot\text{s}^{-1}$ and $100\mu\text{A}\cdot\text{V}^{-1}$.

$E_{pc}, (\text{V})$	i_l, A	i, A	$(i_l - i)/i$	$\log(\text{abs}(i_l - i)/i)$
4.72E-01	3.53E-06	3.53E-06	0.00E+00	undefined
4.77E-01	3.53E-06	3.51E-06	4.70E-03	-2.33
4.82E-01	3.53E-06	3.46E-06	1.81E-02	-1.74
4.87E-01	3.53E-06	3.38E-06	4.24E-02	-1.37
4.92E-01	3.53E-06	3.27E-06	7.87E-02	-1.10
4.97E-01	3.53E-06	3.12E-06	1.30E-01	-0.89
5.02E-01	3.53E-06	2.95E-06	1.97E-01	-0.71
5.07E-01	3.53E-06	2.74E-06	2.87E-01	-0.54
5.12E-01	3.53E-06	2.53E-06	3.96E-01	-0.40
5.17E-01	3.53E-06	2.29E-06	5.39E-01	-0.27
5.22E-01	3.53E-06	2.05E-06	7.22E-01	-0.14
5.27E-01	3.53E-06	1.81E-06	9.49E-01	0.02
5.32E-01	3.53E-06	1.57E-06	1.24E+00	0.04
5.37E-01	3.53E-06	1.35E-06	1.61E+00	0.21
5.42E-01	3.53E-06	1.14E-06	2.09E+00	0.32
5.47E-01	3.53E-06	9.47E-07	2.72E+00	0.44
5.52E-01	3.53E-06	7.74E-07	3.55E+00	0.55
5.57E-01	3.53E-06	6.20E-07	4.69E+00	0.67
5.62E-01	3.53E-06	4.82E-07	6.31E+00	0.80
5.67E-01	3.53E-06	3.63E-07	8.70E+00	0.94
5.72E-01	3.53E-06	2.60E-07	1.26E+01	1.10
5.77E-01	3.53E-06	1.71E-07	1.96E+01	1.29
5.82E-01	3.53E-06	9.46E-08	3.63E+01	1.56
5.87E-01	3.53E-06	2.96E-08	1.18E+02	2.07
5.92E-01	3.53E-06	-2.66E-08	-1.34E+02	2.13
5.97E-01	3.53E-06	-7.42E-08	-4.85E+01	1.69
6.02E-01	3.53E-06	-1.14E-07	-3.19E+01	1.50
6.07E-01	3.53E-06	-1.49E-07	-2.47E+01	1.39
6.12E-01	3.53E-06	-1.79E-07	-2.07E+01	1.32
6.17E-01	3.53E-06	-2.04E-07	-1.83E+01	1.26
6.22E-01	3.53E-06	-2.26E-07	-1.66E+01	1.22
6.27E-01	3.53E-06	-2.45E-07	-1.54E+01	1.19
6.32E-01	3.53E-06	-2.61E-07	-1.45E+01	1.16
6.37E-01	3.53E-06	-2.77E-07	-1.37E+01	1.14
6.42E-01	3.53E-06	-2.90E-07	-1.32E+01	1.12
6.47E-01	3.53E-06	-3.03E-07	-1.26E+01	1.10
6.52E-01	3.53E-06	-3.15E-07	-1.22E+01	1.09
6.57E-01	3.53E-06	-3.27E-07	-1.18E+01	1.07
6.62E-01	3.53E-06	-3.38E-07	-1.14E+01	1.06
6.67E-01	3.53E-06	-3.48E-07	-1.11E+01	1.05
6.72E-01	3.53E-06	-3.60E-07	-1.08E+01	1.03
6.77E-01	3.53E-06	-3.71E-07	-1.05E+01	1.02
6.82E-01	3.53E-06	-3.85E-07	-1.02E+01	1.01
6.87E-01	3.53E-06	-3.99E-07	-9.83E+00	9.93

When applying the experimental data to a plot E_{pa} vs. $\text{Log}((i_l - i)/i)$, a straight line is obtained, (refer to figure 32.a and 32.b) which represent the linear regression for the data. For Cu (II) ions solution the straight line obtained is $y = 15.631x - 2.308$, with slope $m = 15.631$ and with a $R^2 = 0.998$ (Fig. 32.a). For Fe (III) ion solution the strait line obtained is $y = 16.138x - 2.4037$, with slope $m = 16.138$ and with a $R^2 = 0.997$ (Fig. 32.b). From the slope of the lines we can calculate the number of electrons transferred in the reduction process.

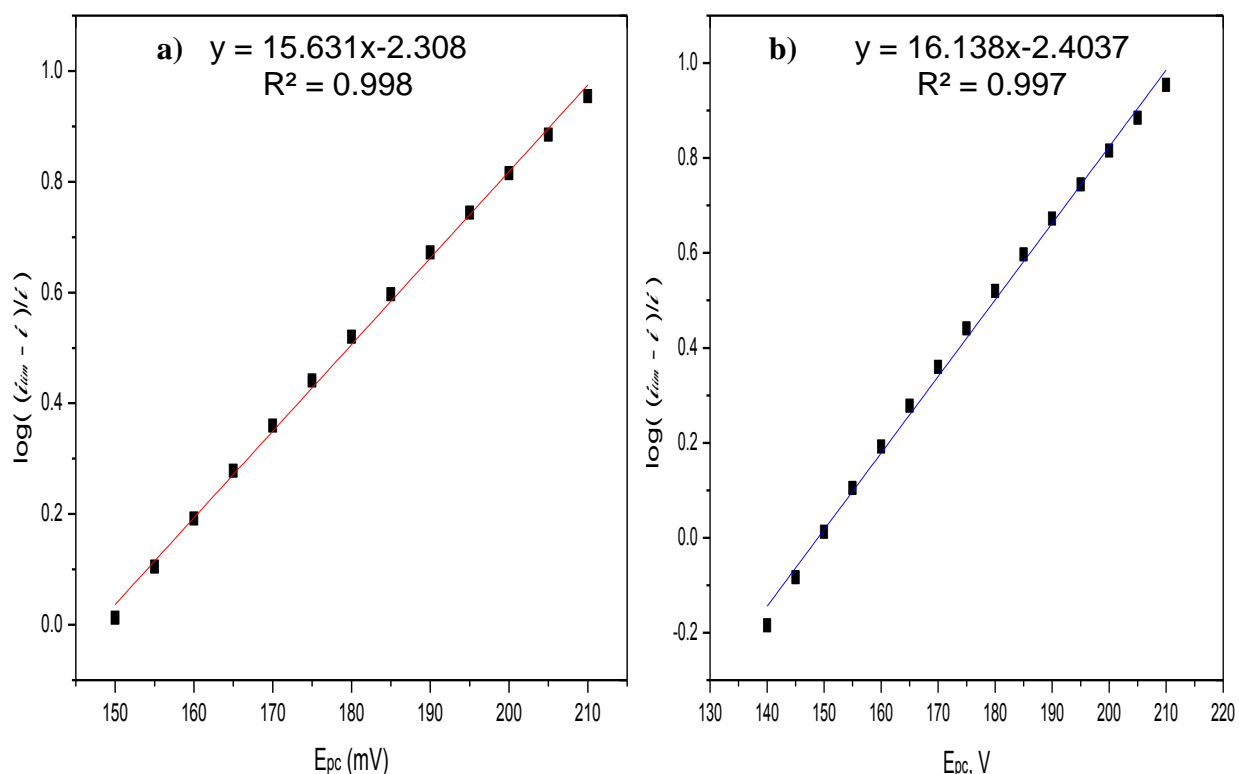


Figure 32. **a)** E_{pa} vs. $\text{Log}((i_l - i)/i)$ plot for the reduction process of 1mM Cu²⁺ in 0.1M NaCl electrolyte supporting solution. The measurement were taken against Ag/AgCl reference electrode at 100mV·s⁻¹ and 100μAV⁻¹ in the +300mV to -100mV potential window **b)** E_{pa} vs. $\text{Log}((i_l - i)/i)$ plot for the reduction process of 1mM Fe³⁺ in 0.1M NaCl electrolyte supporting solution. The measurement were taken against Ag/AgCl reference electrode at 100mV·s⁻¹ and 10μAV⁻¹ in the +700mV to +300mV potential window.

The number of electrons (n) involved in the reduction process was calculated solving the following equation: $n = \left(\frac{2.3mRT}{F} \right)$, and substituting the obtained slope value for Cu (II) ion solution (m = 15.631), the value obtained for the electron transfer was one.

$$n = - \left(\frac{2.3(15.631)(8.314 \text{ Jmol}^{-1} \text{ K}^{-1})(298.16 \text{ K})}{(96,485 \text{ Cmol}^{-1})} \right) = 0.924 \approx 1.0 \quad (18)$$

The number of electrons transfer for Fe (III) obtained from the slope (m = 16.138) was also one electron.

$$n = - \left(\frac{2.3(16.138)(8.314 \text{ Jmol}^{-1} \text{ K}^{-1})(298.16 \text{ K})}{(96,485 \text{ Cmol}^{-1})} \right) = 0.954 \approx 1.0 \quad (19)$$

5.8 Determination of Cu (II) and Fe (III) concentration in Mayaguez Coast seawater using the Standard Addition Method with Cyclic Voltammetry Technique.

A simple calibration curve does not allow the analysis of trace metal in seawater using Cyclic Voltammetry. Due to the fact that the Cyclic Voltammetry technique have about 50% error when using a simple calibration curve at micro Molar scale, the standard addition was selected to analyze the trace metal concentration in naturals.

The use of standard addition method allows quantifying with better accuracy the concentration of Cu (II) and Fe (III) ions in seawater. The seawater used was from the Mayaguez coast. At the selected sensitivity of $1 \mu\text{AV}^{-1}$ the voltammograms of seawater that contain small trace of Cu (II) and Fe (III) do not exhibit any significant peaks, as shown on figure 33.a and 33.b. A potential window from +1000mV to -1000mV or +700mV to +300 mV was used to determine whether or not any other metal peak will be observed.

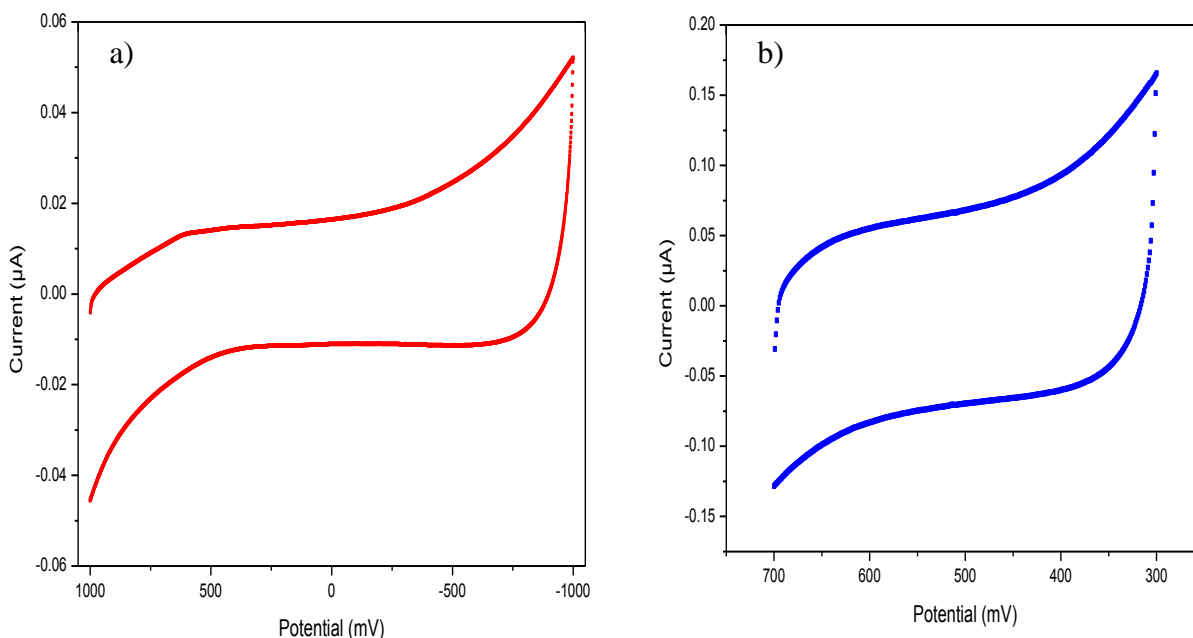


Figure 33. Voltammogram of Seawater analysis **a)** at a scan rate of 100mVs^{-1} and a sensitivity of $100\mu\text{AV}^{-1}$ using **GC working electrode** vs. Ag/AgCl reference electrode, **b)** at a scan rate of 100mVs^{-1} and a sensitivity of $100\mu\text{AV}^{-1}$ using **Pt working electrode** vs. Ag/AgCl reference electrode.

However, subsequent addition of 5 microlites (spikes) of a known concentration (1mM) of Cu(II) or Fe(III) ion solution to the analyzed seawater sample, generate a linear plot of peak current versus added concentration of the standard (spike). Extrapolate in the plot to zero allow to determine the concentration of the unknown solution. Figure 34 and 35 represent the consecutive addition of 5 μL of a 1mM Cu (II) or Fe (III) ions stock solutions, respectively. A total of three samples were analyzed in triplicate. For Cu (II) ion solution the cathodic current was measured at a selected potential of 85mV (refer to table 9) while for Fe (III) the cathodic current was measured at the selected potential of 479mV (refer to table 9). The data obtained is summarized in table 11 and 12.

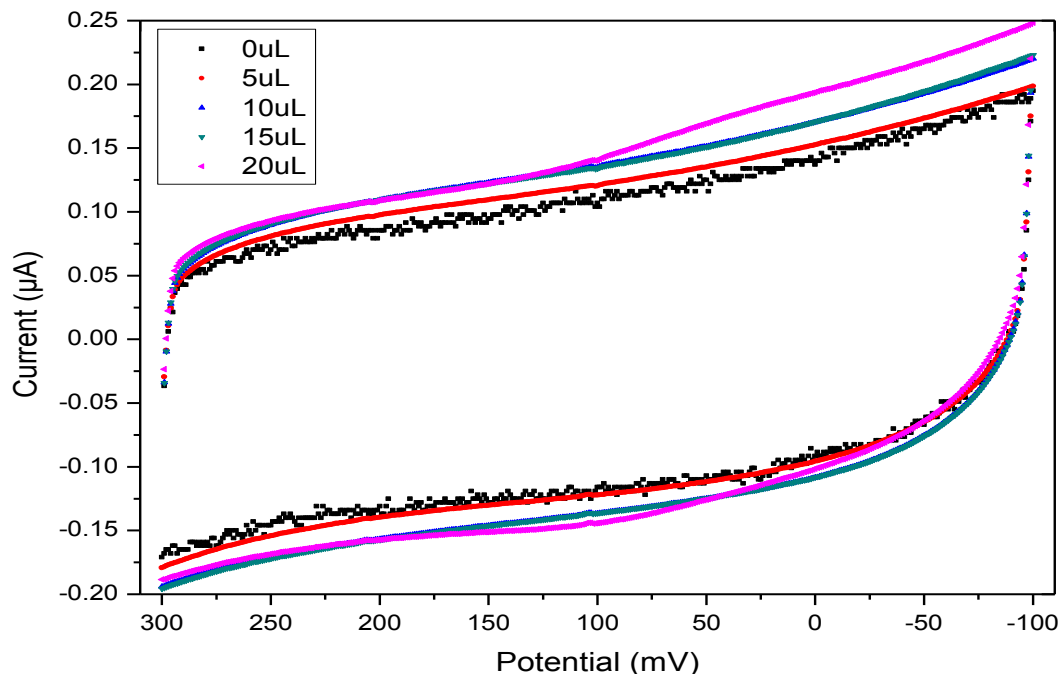


Figure 34. Voltammogram of sea water at every addition of 5uL of 1mM Cu (II) stock solution at a scan rate of 100mVs^{-1} and a sensitivity of $1\mu\text{AV}^{-1}$ vs. Ag/AgCl as reference electrode and using CG working electrode toward a more negative direction.

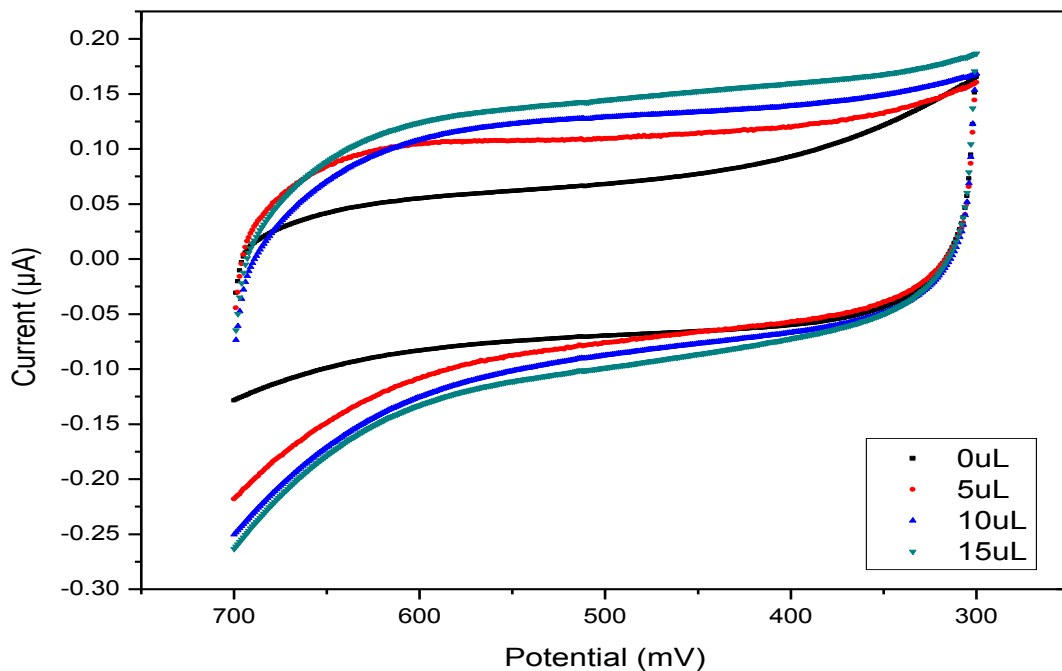


Figure 35. Voltammogram of sea water at every addition of 5uL of 1mM Fe (III) solution at a scan rate of 100mVs^{-1} and a sensitivity of $1\mu\text{AV}^{-1}$ vs. Ag/AgCl as reference electrode and using Pt working electrode toward a more negative direction.

Table11. Summarize of the Cu (II) ion analysis using Standard Addition Method.

Run	Added Volume 1 mM Cu (II) (μ L)	Added Concentration (μ M)	i_{pc} (μ A) at 75mV
1	0	unknown	0.124
	5	0.5	0.140
	10	1.0	0.144
	15	1.5	0.150
2	0	unknown	0.117
	5	0.5	0.135
	10	1.0	0.148
	15	1.5	0.156
3	0	unknown	0.126
	5	0.5	0.136
	10	1.0	0.138
	15	1.5	0.148

Table12. Summarize of the Fe (III) ion analysis using Standard Addition Method.

Run	Added Volume 1 mM Cu (II) (μ L)	Added Concentration (μ M)	i_{pc} (μ A) at 479mV
1	0	unknown	0.0714
	5	0.5	0.112
	10	1.0	0.131
	15	1.5	0.148
2	0	unknown	0.0697
	5	0.5	0.110
	10	1.0	0.125
	15	1.5	0.135
3	0	unknown	0.0685
	5	0.5	0.125
	10	1.0	0.135
	15	1.5	0.150

Table 13 shows average values for the cathodic current used to generate the plot of average cathodic current versus added concentration. The linear behavior for Cu (II) ion in seawater, (refer to fig. 36), generate a straight line $y = 0.0193x (\pm 0.0004) + 0.124 (\pm 0.001)$, with $R^2 = 0.9984$, while for Fe (III) ion (refer to fig. 37) has a straight line $y = 0.052x (\pm 0.005) + 0.074 (\pm 0.003)$ with $R^2 = 0.977$. Both plots have a good linear coefficient. Extrapolating the values we calculate that the concentration of Cu (II) and Fe (III) ions are 8.9 μM and 1.4 μM , respectively. The relative standard deviation for Cu (II) and Fe (III) ions are ± 0.0004 and ± 0.0005 , respectively. Low %RSD were obtained indicating small spread of obtained results.

Table 13. Average of the cathodic current for Cu (II) and Fe (III) ion analysis using standard addition method with Cyclic Voltammetry technique.

Ion	Added Volumen 1 mM (μL)	Added Concentration (μM)	Average i_{pc} (μA) at 85mV	SD	RSD%	R^2
Cu (II)	0	unknown	0.122	0.005	1.3	0.9984
	5	0.5	0.137	0.003	0.6	
	10	1.0	0.143	0.005	1.2	
	15	1.5	0.151	0.004	0.9	
Fe (III)	0	unknown	0.0699	0.001	2.1	0.9388
	5	0.5	0.116	0.008	7.0	
	10	1.0	0.130	0.005	3.9	
	15	1.5	0.144	0.008	5.6	

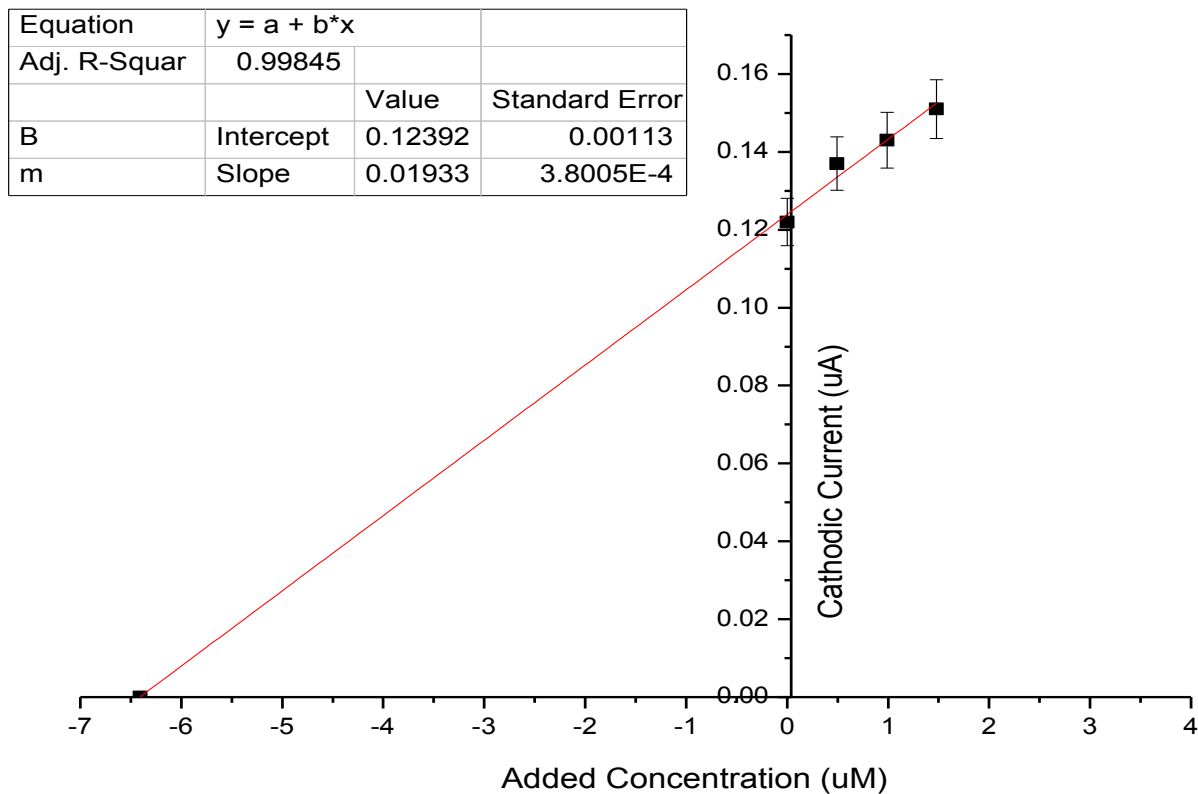


Figure 36. Standard Addition plot for the sample #2 of Cu (II) ion analysis in Mayaguez coast seawater using Cyclic Voltammetry Technique.

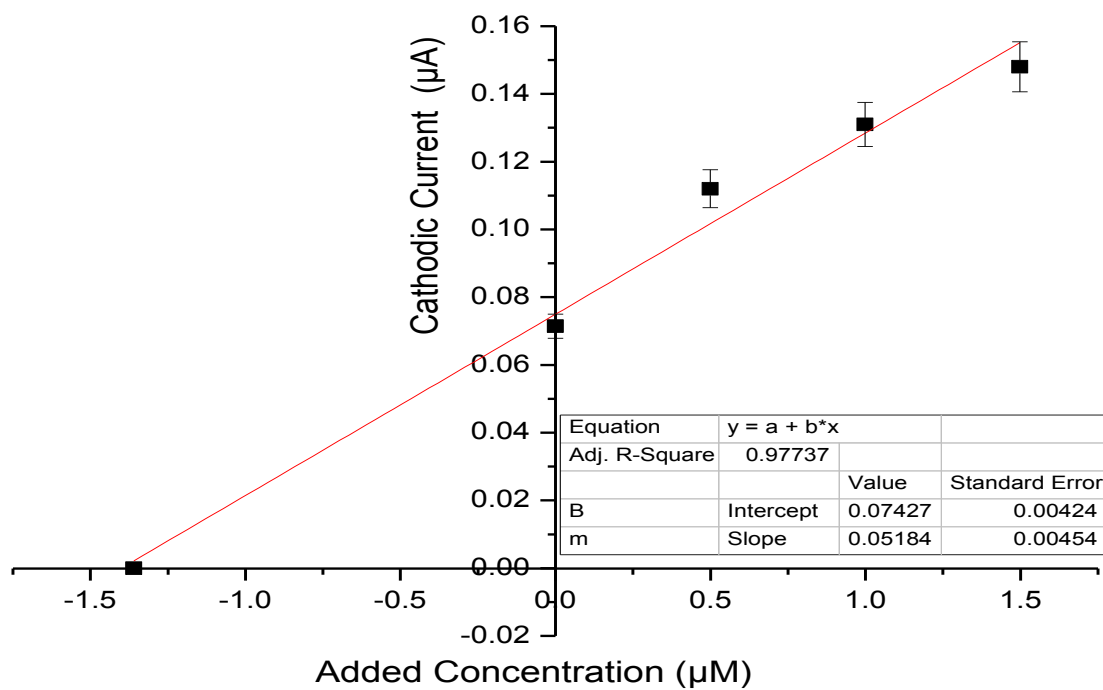


Figure 37. Standard Addition plot for the sample #2 of Fe (III) ion analysis in Mayaguez coast seawater using Cyclic Voltammetry Technique.

Natural water samples were analyzed in triplicates. Table 14 summarizes the data obtained. Data obtained were plotted and extrapolated to determine the content of these two ions. The Mayaguez coast seawater have an average of 7.7 (± 1.0) μM Cu (II) and 1.7 (± 0.4) μM Fe (III) ions concentrations with a standard deviation of $\pm 1.2 \times 10^{-6}$ and $\pm 3.5 \times 10^{-7}$, respectively.

Table 14. Determination of Cu (II) and Fe (III) content in three seawater sample using standard addition method with Cyclic Voltammetry technique.

Ion	Sample	Ion Concentration (μM)	Average Ion Concentration (μM)	SD ($\times 10^{-6}$)
Cu (II)	1	8.9	7.7	1.0
	2	6.5		
	3	7.7		
Fe (III)	1	1.7	1.7	0.4
	2	1.4		
	3	2.1		

5.6 Results Validation

In order to determine whether or not selecting a small variation in the peak current voltage selected to determine the current measurement after adding 5 consecutive spike of 5 μL of a 1mM stock solution a $\pm 10\text{mV}$ to the maximum peak current were used and tabulated in table 15. This table 15 summarizes the Cu (II) and Fe (III) ions data obtained for one sample selecting the cathodic current peak voltage of 75mV, 85mV and 95mV versus Ag/AgCl as reference electrode.

Table15. Cathodic current varying the cathodic peak location at three different potential

Ion	Added Volume (μL)	Added Concentration (μM)	Current at 65 mV (μA)	Current at 75 mV (μA)	Current at 85 mV (μA)
Cu (II)	0	0	0.0340	0.0327	0.0311
	5	0.5	0.0399	0.0370	0.0361
	10	1.0	0.0432	0.0410	0.0384
	15	1.5	0.0459	0.0440	0.0410
	20	2.0	0.0486	0.0465	0.0437
	25	2.5	0.0507	0.0488	0.0452
Ion	Added Volume (μL)	Added Concentration (μM)	Current at 469 mV (μA)	Current at 479 mV (μA)	Current at 489 mV (μA)
Fe (III)	0	0	0.083	0.071	0.069
	5	0.5	0.112	0.102	0.111
	10	1.0	0.132	0.131	0.130
	15	1.5	0.150	0.148	0.146
	20	2.0	0.164	0.162	0.160
	25	2.5	0.179	0.178	0.175

The data for Cu (II) ion (refer to fig. 38.a) generate three straight line, one for each potential selected. At a potential of 65mV the straight line obtained was $y = 0.0064x (\pm 0.0005) + 0.0358 (\pm 0.0008)$, with a $R^2 = 0.9606$. At 75mV (refer to fig. 38.b) the straight line obtained was $y = 0.0064x (\pm 0.0004) + 0.0336 (\pm 0.0006)$, with a $R^2 = 0.9789$. At least, at 85mV the straight line has $y = 0.0054x (\pm 0.0005) + 0.0329 (\pm 0.0007)$, with and $R^2 = 0.9638$ (refer to fig. 38.c). Comparing the slope of each plot, extrapolating the value, the concentration of Cu (II) at each potential are $5.6 (\pm 1) \mu\text{M}$, $5.3 (\pm 1) \mu\text{M}$ and $6.0 (\pm 1) \mu\text{M}$, respectively. These results demonstrate that a small variation of the selected potential current peak do not cost a significant change in current due to this variation. Table 16 summarize the data obtained.

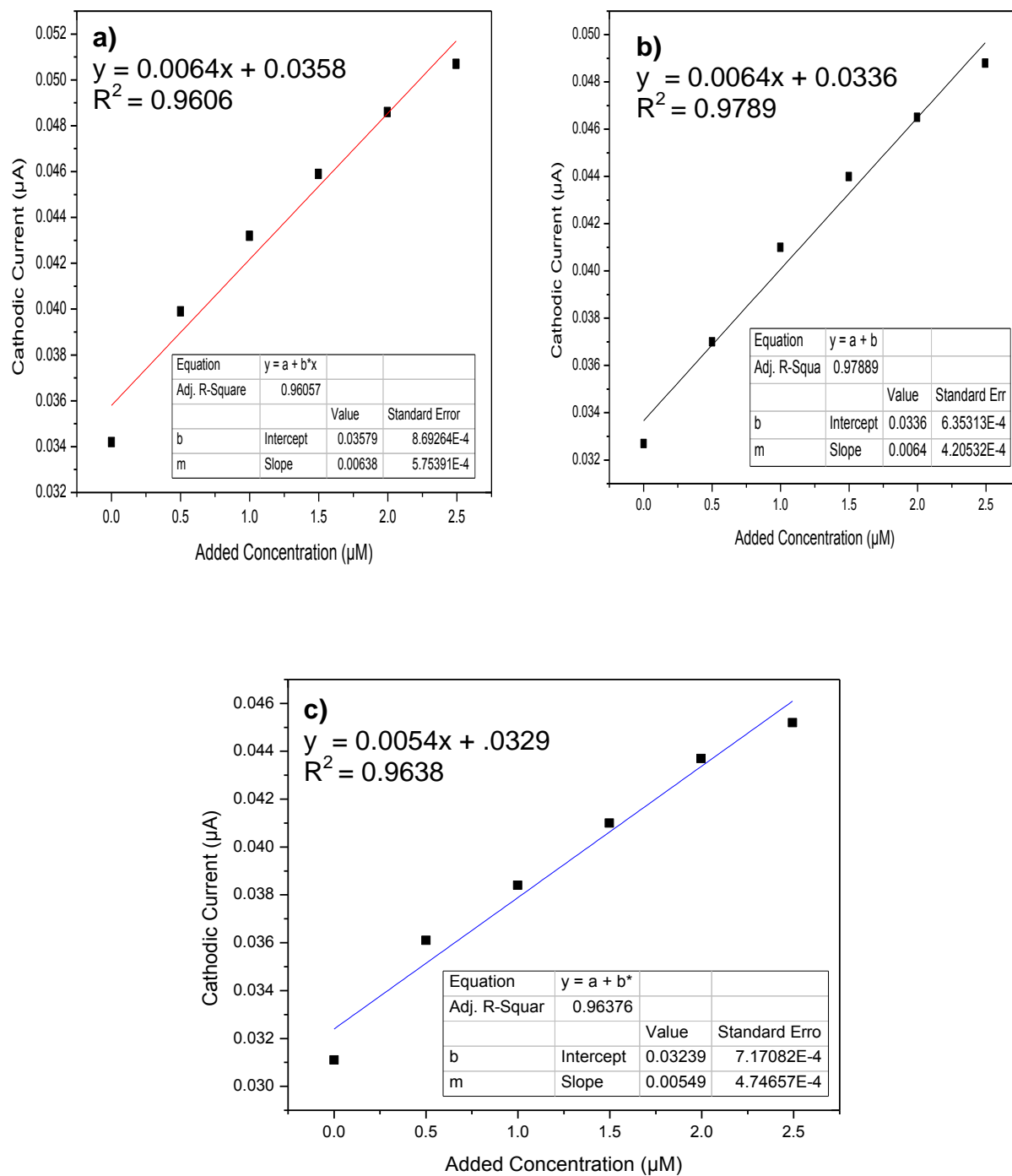


Figure 38. Comparison of the standard addition method plot for Cu (II) ion in the analysis of the Mayaguez coast seawater at small variation in the cathodic current at the potential of **a)** 65 mV, **b)** 75mV and, **c)** 85mV, respectively.

Table.16 Linear regression data for Cu (II) and Fe (III) ion analysis at the selected potentials.

Metal	Potential (mV)	Unknown Concentration (μM)	Straight Line	SD of the Slope	R^2
Cu (II)	65	6.72	$y=0.0064x + 0.0358$	± 0.0005	0.9606
	75	6.68	$y=0.0064x + 0.0336$	± 0.0004	0.9789
	85	6.10	$y= 0.0054x + 0.0329$	± 0.0005	0.9638
Fe (III)	469	2.11	$y=0.037x + 0.090$	± 0.003	0.9769
	479	2.09	$y=0.040x + 0.084$	± 0.004	0.9442
	489	2.10	$y=0.0394x + 0.083$	± 0.005	0.9368

The data for the reduction of Fe (III) ion, (refer to fig. 39.a), generate three straight lines, one at each potential selected versus Ag/AgCl. At a potential of 469mV the straight line obtained was $y = 0.037x (\pm 0.003) + 0.090 (\pm 0.004)$, with and $R^2 = 0.9769$. At 479mV (refer to fig. 39.b) the straight line obtained was $y = 0.040x (\pm 0.004) + 0.084 (\pm 0.007)$, with $R^2 = 0.945$. At 489mV the straight line obtained was $y = 0.039x (\pm 0.005) + 0.083 (\pm 0.007)$, with and $R^2 = 0.9368$ (refer to fig. 39.c). Comparing the slope of each plot, the extrapolate value for the Fe (III) ion concentration in the natural water at each potential were $2.11 (\pm 0.4) \mu\text{M}$, $2.09 (\pm 0.4) \mu\text{M}$ and $2.10 (\pm 0.4) \mu\text{M}$, respectively. Once again, no significant difference was observed. Table 16 summarizes the obtained data.

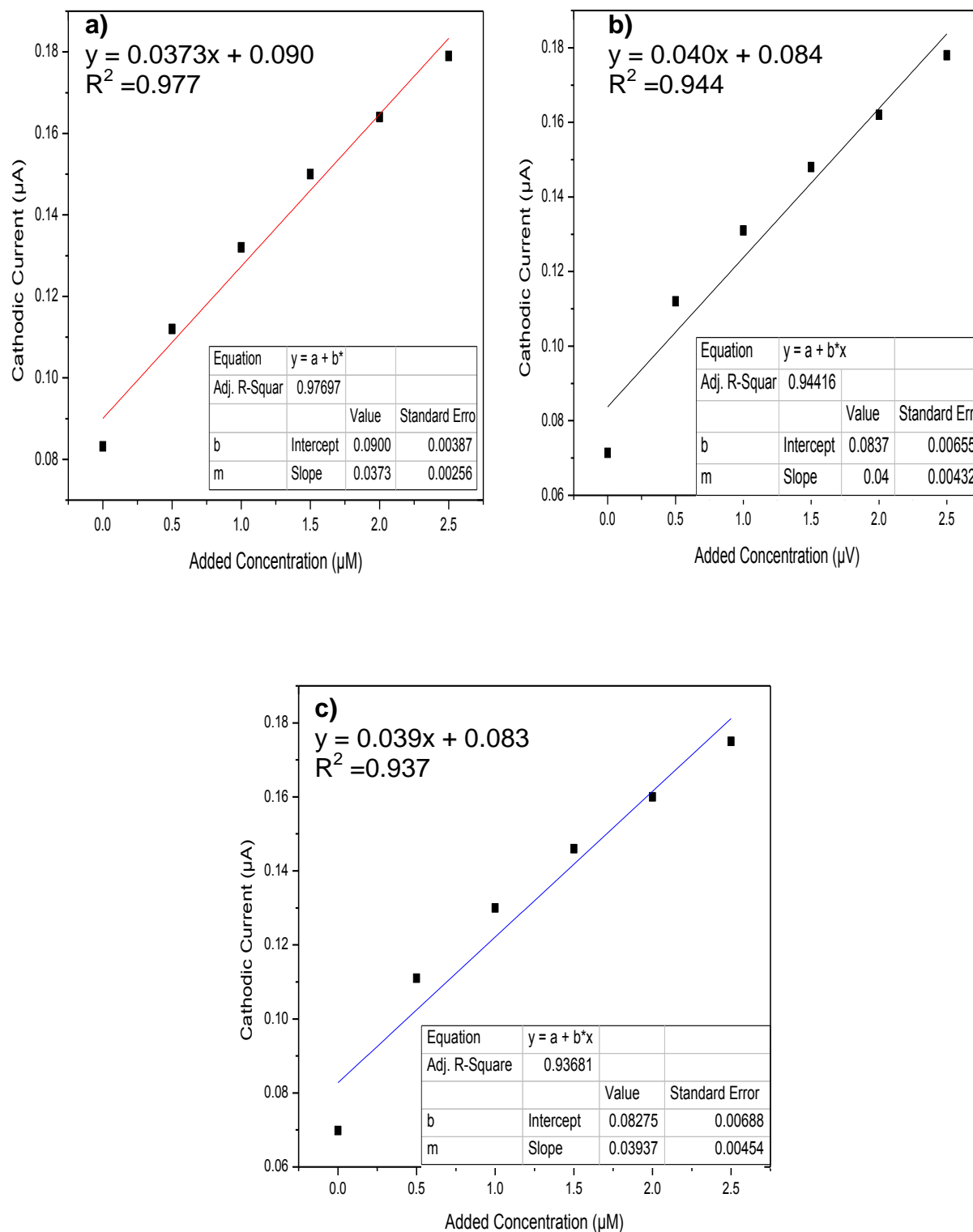


Figure 39. Comparison of three standard addition plot for Fe (III) ion analysis in Mayaguez coast seawater selecting the current the potential at **a)** 469 mV, **b)** 479mV and **c)** 489mV, respectively.

As part of the experimental protocol the volume of the spike and the number of spikes was evaluate. Addition of 1 μ L through 3 μ L of spike do not produced a relevant difference in current measurement in order to quantify the difference between consecutive additions. Otherwise, additions of 1000 μ L (1mL) of spike prove to be too large indicating as shown in figure 26 and table 19 a curve with two distinctive slope (refer to figure 40). One for very low concentration and another one for concentration after two spikes of a 1000 μ L. The appropriate spike volume for the trace analysis of these metals was additions of 5 μ L spike of 1mM stock solution with this Cyclic Voltammetry technique. Table 17 show the data for an experiment of Cu (II) adding spike of mL of volume.

Table 17. Results of the Cu (II) ion analysis using Standard Addition Method with addition of mL of spike.

Volumen (mL)	Added Concentration (mM)	Cathodic Potential (mV)	Cathodic Current (μA)	Anodic Potential (mV)	Anodic Current (μA)
0	Unknown	130	0.550	227	-0.570
1	0.091	130	2.286	227	-1.486
2	0.167	145	5.667	237	-5.042
4	0.286	135	21.885	237	-20.996
6	0.375	125	32.813	237	-32.062
8	0.444	115	45.066	236	-42.084
10	0.500	105	51.0656	238	-46.583

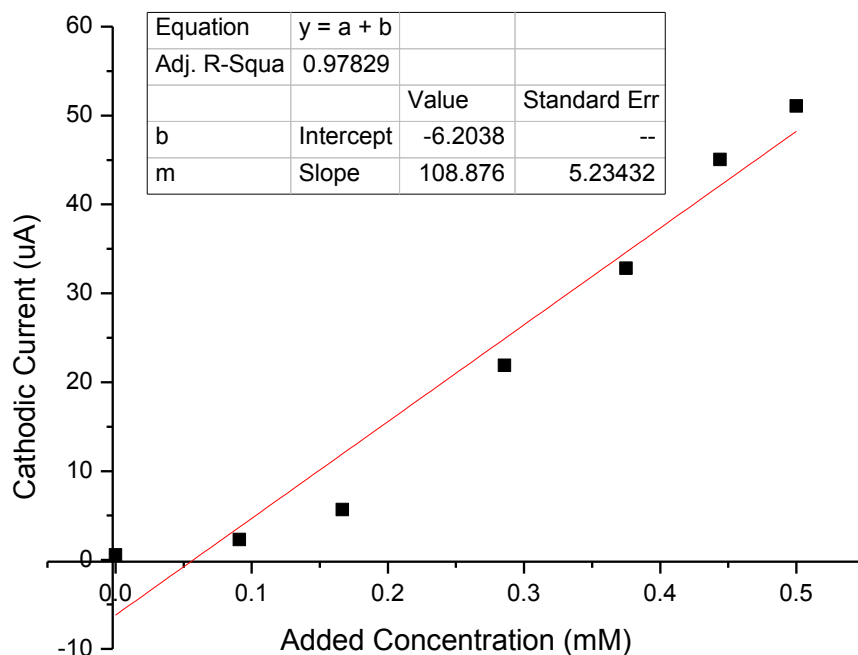


Figure 40. Standard Addition Plot of seawater analysis using 1000 μ L spike of 1mM Cu (II) Stock solution.

Mathematical treatment using a total of 3 or 5 spikes of 5 μ plot in order to determine if there was any difference in the determination of the unknown concentration in natural water. Figure 41 shows the standard Addition plot for Cu (II) ion analysis in Mayaguez coast seawater at 75mV using three spikes addition. Using 3 spikes we obtained a straight line: $y = 0.0076x (\pm 0.0004) + 0.0330 (\pm 0.0004)$. The extrapolate value for Cu (II) concentration was 4.3 μ M. These values have a 25% difference (1.0 μ M) of the concentration obtained when 5 spikes were plotted (refer to figure 38.b).

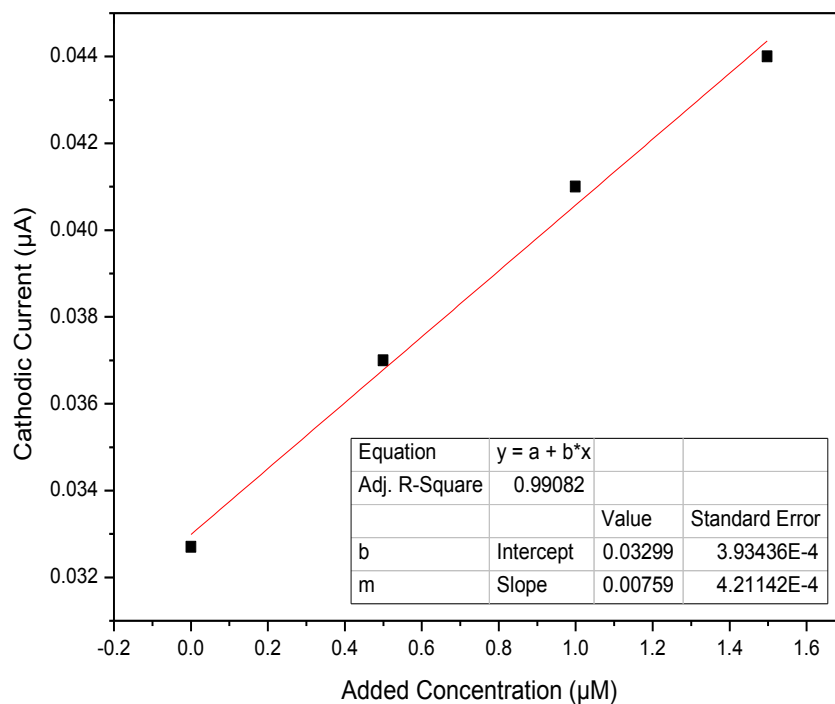


Figure 41. The standard addition plot for Cu (II) ion analysis in Mayaguez coast seawater at 85mV using 3 spikes addition.

For Fe (III), figure 42 shows the standard Addition plot for Fe (III) ion analysis in Mayaguez coast seawater at 479mV using three spikes addition. Using 3 spikes we obtained a straight line: $y = 0.0049x (\pm 0.007) + 0.078 (\pm 0.007)$. The extrapolate value for Fe (III) concentration was 1.6 μM . These values have a 6% difference (0.1 μM) of the concentration obtained when 5 spikes were plotted (refer to figure 39.b).

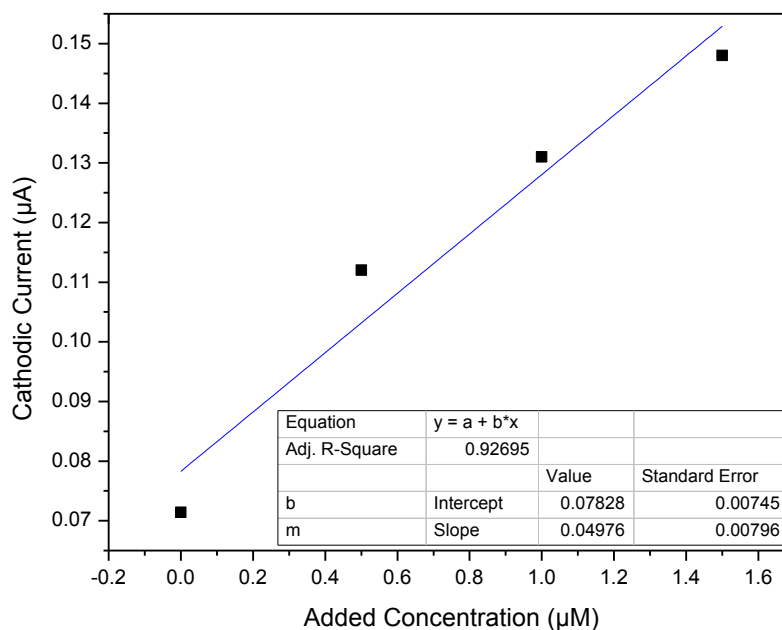


Figure 42. The standard addition plot for Fe (III) ion analysis in Mayaguez coast seawater at 479mV using 3 spikes addition.

To corroborate the accuracy of the results, a 1μM Cu (II) stock solution and a 1μM Fe (III) stock solution were analyzed using the standard addition method. Table 18 shows the data recollected for each of the ions.

Table 18. Average Results of the 1μM Cu (II) and 1μM Fe (III) stock solution analysis.

Metal	Potential (mV)	Added Concentration (μM)	Unknown Concentration (μM)	Straight Line	R ²
Cu (II)	85	0	0.034	$y = 0.041x + 0.034$	0.9976
		0.5	0.053		
		1.0	0.076		
		1.5	0.095		
Fe (III)	479	0	0.0701	$y = 0.0612 x + 0.069$	0.9932
		0.5	0.1005		
		1.0	0.1205		
		1.5	0.1599		

Figure 43 shows the standard Addition plot for 1 μM Cu (II) stock solution at 85mV using three spikes addition and CG working electrode. We obtained a straight line: $y = 0.041 (\pm 0.001)x + 0.034 (\pm 0.001)$ with a linear regression $R^2 = 0.9976$. The extrapolate value for Fe (III) stock solution concentration was 0.82 μM . These values have a 18% of difference of the original concentration.

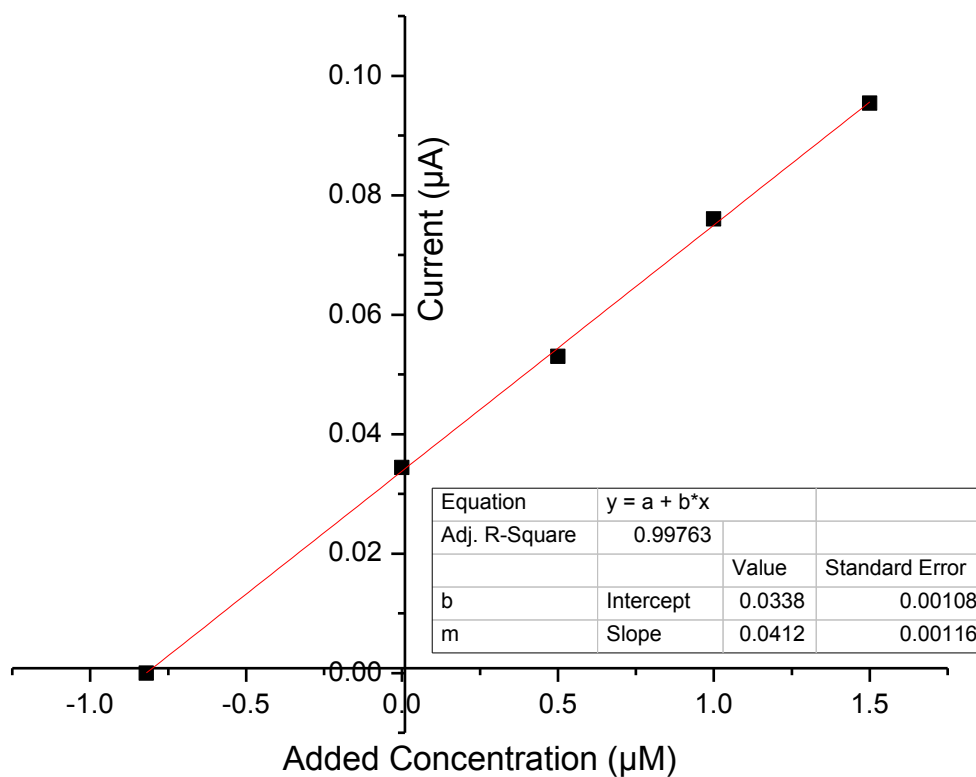


Figure 43. The standard addition plot for 1 μM Cu (II) stock solution at 75mV using 3 spikes addition and GC working electrode.

Figure 44 shows the standard Addition plot for 1 μ M Fe (III) stock solution at 479mV using three spikes addition and Pt working electrode. We obtained a straight line: $y=0.061x (\pm 0.003) + 0.069 (\pm 0.003)$ with linear regression $R^2 = 0.9931$. The extrapolate value for Fe (III) stock solution concentration was 1.13 μ M. These values have a 13% difference of the original concentration.

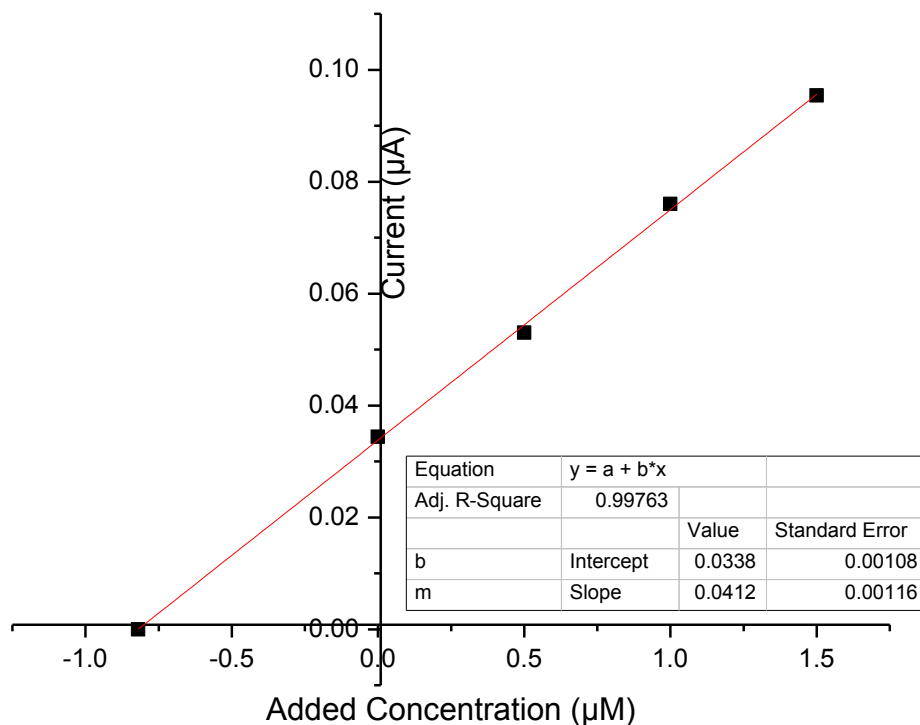


Figure 44. The standard addition plot for 1 μ M Fe (III) stock solution at 479mV using 3 spikes addition and Pt working electrode.

Chapter VI: Conclusions and Recommendations

6.1 Conclusions

Our research aimed to determine whether or not the Cyclic Voltammetry technique allow to determine trace (micromolar, μM) concentration of Cu(II) and Fe (III) ion in natural waters using the Standard Addition Method. Several experimental protocols were done in order to identify the proper experimental design for the analysis with the lower experimental error. After choosing the proper protocol we proceed focusing on the convenience of the use of standard addition method combine with Cyclic Voltammetry technique. This combination of methods was validated with different range of spike additions. Our results indicate that the levels of Cu (II) and Fe (III) ions concentration in the seawater of Mayaguez coast were $7.7 (\pm 1) \mu\text{M}$ and $1.7 (\pm 0.4) \mu\text{M}$, respectively. The pH and salinity measured of the seawater of Mayaguez coast were 8.07 and 26.42 mgL^{-1} , respectively. Our results demonstrate that this technique is suitable for the analysis of ion trace metal concentration of Cu (II) and Fe (III). The optimal instrumental parameters for this analysis were determined and reported in this thesis: Several different metal electrode were tested and glassy carbon is recommended as the ideal one for analysis of Cu (II) ion and for the analysis of Fe (III) the ideal electrode surface was determined to be Platinum. Potential window determined for Cu (II) ion with the GC working electrode was between +300mV to -100mV, a scan rate of 100 mVs^{-1} and a Sensitivity of $1 \mu\text{AV}^{-1}$ versus Ag/AgCl as reference electrode. While for the Fe (III) ion analysis using Pt working electrode the potential window was between +700mV to +300mV, a scan rate of 100 mVs^{-1} and a sensitivity of $1 \mu\text{AV}^{-1}$ versus Ag/AgCl as reference electrode.

6.2 Recommendation for future work

With the protocol and parameters determined and recommended it is possible to focus to the analysis of other trace metal ions of importance for the life cycle in natural waters. It is also recommended to study Cu (II) and Fe (III) ions at different seawater depths in order to determine if there are any variations as a function of depth.

The quantities of trace metal in the seawater surface depend of the redox processes that are occurring due to the presence of oxidizing or reducing agents. Hydrogen peroxide is a redox agent and their seawater concentration is increasing due to the high level of irradiation of solar light. H_2O_2 can reduce the concentrations of Cu (I) and Fe (III) in the seawater surface. Therefore, the level of these trace metal in the seawater should be less than their levels in depth seawater. The level of these ions in surface seawater can be monitor and correlate to the global warming.

Other researches in our laboratory have been developing protocols for the determination of the kinetic of the reaction of hydrogen peroxide and Cu (II) ion and Fe (III) in seawater using multiple cycle experiments with Cyclic Voltammetry. The data obtained with our research reported here is complementary with the kinetic experiment. The information obtain can be of importance for the scientific community in order to protect life cycle in natural waters.

References

1. Bard, A.J.; Faulkner, L.R. Electrochemical Methods: Fundamentals and Applications. New York: John Wiley & Sons, 1980
2. A. W. Bott, Ph.D. Practical Problems in Voltammetry: 4. Preparation of Working Electrodes. www.Basinc.com
3. C. M. G. van den Berg. Direct Determination of Molybdenum in Seawater by Adsorption Voltammetry. *Analytical Chemistry*. 1985, 57, 8.
4. D. A. Segar and A. Y. Cantillo. Direct Determination of Trace Metals in Seawater by Flameless Atomic Absorption Spectrophotometry. *Analytical Methods in Oceanography Advances in Chemistry*. 1975, Vol. 147, Chapter 7, 56–81.
5. E. P. Achterberg and Ch. Braungardt. Stripping voltammetry for the determination of trace metal speciation and in-situ measurements of trace metal distributions in marine waters. *Analytica Chimica Acta* 400. 1999 381–397.
6. E. P. Achterberg, Ch. B. Braungardt, and K. A. Howell. Field Application of an Automated Voltammetric System for High-Resolution Studies of Trace Metal Distributions in Dynamic Estuarine and Coastal Waters. *Environmental Electrochemistry*. 2002 Vol. 811 Chapter 5, 73–101.
7. F. J. Millero, R. L. Johnson, C. A. Vega, K. Sharma, I and S. Sotolonsor. Effect of Ionic Interactions on the Rates of Reduction of Cu (II) with H_2O_2 in Aqueous solutions. *Journal of Solution Chemistry*. 1992, 21, 12.
8. H. E. Allen, W. R. Matson and K. H. Mancy. Trace metal characterization in aquatic environments by anodic stripping voltammetry. *Water Pollution Control Federation*. 1970, 42.
9. L.M. Laglera and C. M. G. van der Berg. Wavelength Dependence of the Photochemical Reduction of Iron in Arctic Seawater. *Environmental Science Technology*. 2007, 41, 2296-2302.
10. J. Buffle, M.-L. Tercier-Waebe. Voltammetric environmental trace metal analysis and speciation: from laboratory to in situ measurements. *Trends in Analytical Chemistry* .2005, 24, 3.

11. J. Nishioka, S. Takeda, H. J.W. de Baar, P.L. Croot, M. Boye, P. Laan, K. R. Timmermans. Changes in the concentration of iron in different size fractions during an iron enrichment experiment in the open southern Ocean. *Marine Chemistry*. 2005, 95, 51- 63.
12. J. W. Moffett and R. G. Zika. Reaction Kinetics of Hydrogen Peroxide. *Environmental Science Technology*. 1987, 21, 8, 804-810.
13. L.M. Laglera and C. M. G. van der Berg. Wavelength Dependence of the Photochemical Reduction of Iron in Arctic Seawater. *Environmental Science Technology*. 2007, 41, 2296-2302.
14. M. González-Dávila, J. M. Santana-Casiano, A.G. González, N. Pérez, and F.J. Millero. Oxidation of copper(I) in seawater at nanomolar levels. *Marine Chemistry* 2009, 115, 118–124.
15. M. Vega and C. M. G. van den Berg. Determination of Cobalt in Seawater by Catalytic Adsorptive Cathodic Stripping Voltammetry. *Analytical Chemistry*. 1997, 69, 874-881.
16. P. Figural and B. McDuffie. Determination of Labilities of Soluble Trace Metal Species in Aqueous Environmental Samples by Anodic Stripping Voltammetry and Chelex Column and Batch Methods. *Analytical Chemistry*. 1980, 52, 9, 1433-1439.
17. S. H. Lieberman and A. Zirino. Anodic Stripping Voltammetry of Zinc in Seawater with a Tubular Mercury-Graphite Electrode. *Analytical Chemistry*. 1974, 46, 1. 20-23.
18. V. A. Elrod, K. S. Johnson,* and K. H. Coale. Determination of subnanomolar Levels of Iron(II) and Total Dissolved Iron in Seawater by Flow Injection Analysis with Chemiluminescence Detection. *Analytical Chemistry*. 1991, 63, 9, 893-898.
19. W. Rudolf Seitz, W. W. Suydam and D. M. Hercules. Determination of Trace Amounts of Chromium(III) Using Chemiluminescence Analysis. *Analytical Chemistry*. 1972, 44, 6, 957-963.
20. W. Sung* and J. J. Morgan. Kinetics and Product of Ferrous Iron Oxygenation in Aqueous Systems. *Environmental Science & Technology*. 1980, 14, 5.

21. X. Liu and F. J. Millero. The solubility of iron in seawater. *Marine Chemistry*. 2002, 77, 43- 54.
22. J. Orozco, C. Fernandez-Sanchez and C. Jimenez-Jorquera. Underpotential Deposition-Anodic Stripping Voltammetric Detection of Copper at Gold Nanoparticle-Modified Ultramicroelectrode Arrays. *Environmental. Science Technology*. 2008, 42, 4877–4882
23. G. González, J. M. Santana-Casiano, and M. González-Dávila .Oxidation of Copper(I) in seawater at nanomolar levels. *Marine Chemistry*. 2009, Vol. 115, Issues 1-2, pp. 118-124
24. S. J. Ussher, A. Milne, W. M. Landing, K. Attiq-ur-Rehman, M. J.M. Séguret, T. Holland, E. P. Achterberg, A. Nabi and P.I.J. Worsfold. Investigation of iron(III) reduction and trace metal interferences in the determination of dissolved iron in seawater using flow injection with luminal chemiluminescence detection. *Analytica Chimica Acta*. 1999 Vol. 652, Issues 1-2, pp. 259-265
25. J. M. Santana-Casiano, M. González-Dávila, and F.J. Millero. Oxidation of Nanomolar Levels of Fe(II) with Oxygen in Natural Waters. *Environmental Science. Technology*. 2005, 39 (7), 2073–2079.
26. Skoog, Holler & Nieman. *Principios de Análisis Instrumental*. Chapter 25, (1992), Ed.5
27. Windsor Sung* and James J. Morgan. Kinetics and Product of Ferrous Iron Oxygenation in Aqueous Systems. *ACS*. (1980) Vol. 14, No 5, pp.561-568
28. W Davison, G Seed. The kinetics of the oxidation of ferrous iron in synthetic and natural waters. *Geochimica et Cosmochimica Acta*. (1983), Volu 47, Issue 1, pp. 67-79.
29. Frank J Millero. The effect of ionic interactions on the oxidation of metals in natural waters. *Geochimica et Cosmochimica Acta*. (1985), Vol. 49, Issue 2, pp. 547-553
30. Haber, F.; Weiss, J. J. *Proc. R. SOC. London, A* 1934, 147, 332.
31. Barb, W. G.; Baxendale, J. H.; George, P.; Hargrave, K. R. *Trans. Faraday SOC*. 1951, 47, 591-616.

32. W. J. Copper, R. G. Zika, R. G. Petasne, and J. M. C. Plane. Photochemical Formation of H_2O_2 in Natural Waters Exposed to Sunlight. *Environmental Science Technology*. (1988), 22, 1156-1160.
33. C. A. Ribera and C. A. Vega-Olivencia. Electrochemistry studied of the interaction of Iron (II) with peroxide in natural and industrial waters". (2001).
34. Bard and Faulker in *Electrochemical Methods: Fundamentals and Applications*, 2nd, Wiley & Sons, 2001.
35. Vernier LabQuest. Ion Selective Electrode. Beaverton, OR. Rev 10/19/10